You’re your own best teacher: A Self-Supervised Learning Approach For Expressive Representations

Johan Vik Mathisen

May 20, 2024

Abstract

The `ntnuthesis` document class is a customised version of the standard LaTeX `report` document class. It can be used for theses at all levels – bachelor, master and PhD – and is available in English (British and American) and Norwegian (Bokmål and Nynorsk). This document is ment to serve (i) as a description of the document class, (ii) as an example of how to use it, and (iii) as a thesis template.

Sammendrag

Dokumentklassen `ntnuthesis` er en tilpasset versjon av LaTeX' standard `report`-klasse. Den er tilrettelagt for avhandlinger på alle nivåer – bachelor, master og PhD – og er tilgjengelig på både norsk (bokmål og nynorsk) og engelsk (britisk og amerikansk). Dette dokumentet er ment å tjene (i) som en beskrivelse av dokumentklassen, (ii) som et eksempel på bruken av den, og (iii) som en mal for avhandlingen.

Contents

Abstract . . . . . **iii**
Sammendrag . . . . . **v**
Contents . . . . . **vii**
1 Introduction **1**
1.1 Motivation 1
1.2 Overview/structure 2
1.3 Research questions 2
1.4 AI Declaration 2
2 Theoretical Background **3**
2.1 Notation 3
2.2 Information theoretic/basic stats used in evaluation 3
2.3 Time Series Inference 4
2.4 Neural Network 4
2.4.1 Training Neural Networks 5
2.5 Convolutional Neural Network 7
2.5.1 The convolution operation 7
2.5.2 Pooling 9
2.5.3 Architecture 9
2.5.4 Transposed Convolutional Networks 10
2.6 Representation Learning 11
2.6.1 Why do we care about representation learning? 11
2.6.2 What a representation? 12
2.6.3 What is a good representation? 13
2.6.4 How does one evaluate representations? 13
2.7 Transformers 14
2.7.1 The attention mechanism 16
2.7.2 Architecture 17
2.7.3 Bi-directional transformer (BERT) 17
2.8 Self-Supervised learning 17
2.8.1 Supervised 17
2.8.2 Unsupervised 18
2.8.3 Self-supervised 18
2.8.4 Masked modelling 20
2.9 Vector Quantized Variational Autoencoder (VQVAE) 21

2.9.1 Autoencoder (AE) . . . 21
2.9.2 Variational Autoencoder (VAE) . . . 21
2.9.3 Vector Quantization (VQ) . . . 24
2.9.4 VQVAE . . . 24
2.10 Evaluation metrics . . . 27
2.10.1 Tokenization model . . . 27
2.10.2 Generative model . . . 27
3 Related Work . . . 33
3.1 MaskGIT . . . 33
3.1.1 Masked Visual Token Modeling (Prior learning) . . . 33
3.1.2 Iterative decoding (Image generation) . . . 34
3.2 TimeVQVAE . . . 35
3.2.1 Tokenization . . . 36
3.2.2 Prior learning . . . 36
3.3 SSL . . . 36
3.3.1 Barlow Twins . . . 37
3.3.2 VIbCReg . . . 38
4 Methodology . . . 41
4.1 Proposed model: NC-VQVAE . . . 41
4.1.1 NC-VQVAE . . . 42
5 Experiments . . . 43
5.1 Implementation details . . . 43
5.2 Initial Experimentation and Model Development . . . 44
5.3 Main Experiments . . . 45
5.4 Stage 1 . . . 45
5.4.1 Augmentations . . . 45
5.4.2 Evaluation . . . 46
5.5 Stage 2 . . . 46
5.5.1 Evaluation . . . 46
5.6 UCR Time Series Classification Archive . . . 46
6 Results and Discussion . . . 49
6.1 Stage 1 . . . 49
6.1.1 Reconstruction . . . 49
6.1.2 Classification . . . 49
6.2 Stage 2 . . . 49
6.2.1 Thought: . . . 49
6.2.2 Ablation . . . 49
6.2.3 Augmentation Reconstruction Weight . . . 49
6.2.4 Augmentation robustness . . . 50
6.3 Discussion . . . 50
6.4 Further work . . . 51
7 Conclusion . . . 53
7.1 Reconstruction . . . 53
7.2 Classification . . . 53

Bibliography **55**
A Additional Material **59**

Chapter 1

Introduction

In this thesis we investigate possible improvements on the TimeVQVAE model presented by... We investigate how a "self supervised learning extension" of the tokenization affects the learned representations, and the effect on the prior learning. In particular we investigate if the learned representations are more informative, in the sense that they simultaneously enables high quality reconstruction, and improved the downstream classification accuracy. For the generative model we investigate if the learned representations enables faster convergence during training, and how the quality of the synthetic samples are affected.

1.1 Motivation

- The role and importance of time series. - The need for models that capture complex structures for which traditional statistical models fail. Real world time series data is often incomplete (missing datapoints), irregular (datapoints not evenly spaced in time) and noisy. ML4ITS. - - Why do people care about time series generation (TSG)? - Applications - Why is (unsupervised) representation learning for time series interesting? Distributions of time series in their original temporal representation are complex and difficult to model. One would like to translate time series to a space where modelling is easier. This is one of the reasons to investigate representation learning for time series. Time series are recorded at record speed from sensors of various kinds (IoT, wearable devices). Unfortunately many of these do not have easily recognizable patterns for human observers, which makes labeling of such data quite difficult. In order to take advantage of this vast amount of unlabled data we need techniques that can extract useful patterns without supervision. This is one of the reasons for investigating possible unsupervised models. A subcategory of unsupervised learning called self-supervised learning has in recent times shown great potential for learning informative and useful representations without the need of labeled data in the fields of computer vision and natural language processing. Most notably the GPT models from OpenAI which utilizes masked language modelling for pre-training.

1.2 Overview/structure

- Main inspirations [1]
- Collaboration with Erlend
- Structure of the thesis

1.3 Research questions

- Does VQVAE learn good representations for classification? - Will self a supervised learning approach (BT, VIbCReg) enhance the representations learned from VQVAE for classification, and how does is affect the reconstruction? - Will more expressive representations improve prior model learning? - How does SSL VQVAE compare when we train a powerful prior model on top of it (MaskGIT)?

1.4 AI Declaration

- Ethical and environmental impact consideration with basis in UN sustainability goals

Chapter 2

Theoretical Background

TODO: Introduce the section, what we think and the philosophy of presenting material in such a way.

2.1 Notation

- Encoder E
- Decoder D
- Estimated values are presented with a hat, $\widehat{x}$ for a reconstructed value, $\widehat{f}$ for a trained model etc.
- Parameters θ
- Dataset $X = \{x_i\}_{i=1}^{N}$

2.2 Information theoretic/basic stats used in evaluation

- maximum entropy distribution
- mutual information

Definition 1 (Differential entropy) *The differential entropy of a random variable X with pdf or pmf p defined on a sample space $\mathcal{X}$ is*

$$h(X) = \mathbb{E}[-\log(f(X))] - \sum_{x \in \mathcal{X}} p(x)\log(p(x)), \text{ if } X \text{ is discrete,} \tag{2.1}$$

$$h(X) = \mathbb{E}[-\log(f(X))] - \int_{\mathcal{X}} p(x)\log(p(x)), \text{ if } X \text{ is continuous} \tag{2.2}$$

- perplexity

Definition 2 (KL-Divergence) *For probability distribution P and Q defined on the same sample space $\mathcal{X}$, if for all $x \in \mathcal{X}$ $Q(x) = 0$ implies $P(x) = 0$, the Kullback-Leibler divergence is defined as*

$$\mathrm{KL}(P||Q) = \sum_{x \in \mathcal{X}} P(x) \log\left(\frac{P(x)}{Q(x)}\right), \text{ if } P \text{ and } Q \text{ are discrete,} \tag{2.3}$$

$$\mathrm{KL}(P||Q) = \int_x p(x) \log\left(\frac{p(x)}{q(x)}\right) dx, \text{ if } P \text{ and } Q \text{ are continuous.} \tag{2.4}$$

`https://stats.stackexchange.com/questions/188903/intuition-on-the-kullback-leibler-kl-189758#189758`

- Cross entropy
- Graphical probabilistic models - Ancestral sampling
- Generative models

2.3 Time Series Inference

- short-time-fourier transform etc.

2.4 Neural Network

An *artificial neural network* or simply *neural network* is a fundamental model in machine learning, and more specifically in *deep learning*. Neural networks are loosely inspired by the way neurons are assembled in the brain. The model can be traced back the year of 1943 when Warren McCulloch and Walter Pitts developed the first artificial neuron [2], which is considered to be the first neural model invented. It was first set out in the real world by Frank Rosenblatt in 1957 [3]. But not until the development of the backpropagation algorithm in its modern form in the 1980's did the model really gain traction. Neural networks have since then been the highly influential in the development of the machine learning field, with an impressive resume of applications. Some of which, if we stretch the definition a bit, include face recognition, beating humans in chess, Go and Starcraft, self-driving cars and predicting the structure of proteins. The unreasonable effectiveness of neural networks on a broad range of tasks can in part be explained by the *universal approximation theorem*, proven by Kurt Hornlik in 1989 [4], which roughly states that a neural network can approximate any (Borel measurable) function to any desired degree of accuracy.

A neural network takes in a vector $x \in \mathbb{R}^n$ and builds a nonlinear function $f(x)$ to predict the response $y \in \mathbb{R}^m$. More specifically a neural network maps an input vector x to an output vector y through a series of non-linear functions of linear combinations of the input. This particular structure, presented in figure 2.1 is what distinguishes neural networks from other nonlinear prediction models.

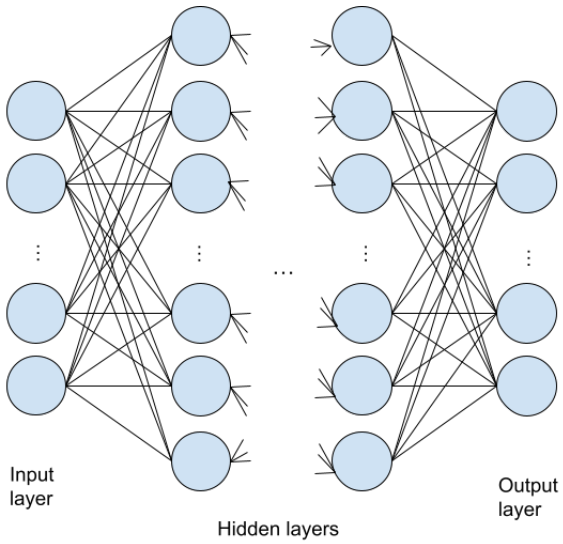

Figure 2.1: Illustration of a Neural Network model.

The variables $x = [x_1, ..., x_n]$ constitutes the units of the *input layer*. The intermediate layers are called the *hidden layers*, and the final mapping to y is called the *output layer*. A neural network is parameterized by a set of *weight* matrices W_i and *bias* vectors b_i, together with a specified non-linear *activation function* σ. We denote the collection of parameters $\{W_1, ..., W_{K-1}, b_1, ..., b_{K-1}\}$ by θ. Written out a K layered neural network is given by

$$f_\theta(x) = f_K \circ f_{K-1} \circ \ldots \circ f_2 \circ f_1(x),$$

where

$$f_i(x) = \sigma(W_i x + b_i), \quad i \in \{1, ..., K-1\},$$

and f_K is the output layer, with application dependent structure.
The introduction of nonlinearity by the activation function is what enables the model to approximate nonlinear signals and differentiate itself from a linear regression model. Two of the most commonly used activation functions are $\text{Sigmoid}(x) = \frac{1}{1+\exp(-x)}$ and $\text{ReLU}(x) = \max(0, x)$, but countless options exists.
The architecture of neural networks, and most specializations thereof, is sequential in nature. They can effectively be described as compositions of some combination of a flavour of matrix multiplication, non-linear transformation and down or upsampling.

2.4.1 Training Neural Networks

The training of a neural network is the process of finding values for the weight and bias parameters. The general idea governing neural network training is to optimize the parameters based on some distance metric between the predicted values and the target values. This distance metric is referred to as the *loss function*, and

a common choice of loss function is the mean squared error (MSE).

For a multi-variable function F which is differentiable around a point a, the direction which it decreases fastest when starting in the point a is given by the negative gradient at a, $-\nabla F(a)$. The gradient descent algorithm utilizes this property to find local minima of F by initializing the function with a value x_0 and iteratively update

$$x_{n+1} = x_n - \gamma \nabla F(x_n).$$

If the *learning rate* γ is small enough we are guaranteed that $F(x_{n+1}) \geq F(x_n)$, and the sequence $x_0, x_1, \ldots$ converge to a local minima of F.

A neural network $f_\theta(x)$ is itself a multi-variable function, and as long as the loss and activation function are differentiable, the network is as well, both in terms of it argument and parameters. If one differentiates the network with respect to its parameters across its domain, the negative gradient indicates the fastest direction in which to update the parameters to minimize the loss. The optimization problem at hand, for a dataset $X = \{x_i\}_{i=1}^N$ with corresponding labels $Y = \{y_i\}_{i=1}^N$, is

$$\widehat{\theta} = \min_\theta \frac{1}{N} \sum_{i=1}^{N} \mathcal{L}(f_\theta(x_i), y_i),$$

and one would iteratively update the parameters by gradient descent

$$\theta_{n+1} = \theta_n - \frac{\gamma}{N} \sum_{i=1}^{N} \nabla_\theta \mathcal{L}(f_\theta(x_i), y_i).$$

If the dataset X is large, the gradient calculations are expensive. In these cases, which in modern machine learning is the standard scenario, an effect estimator for the true gradient is used instead. Stochastic gradient descent (SDG) is a very popular approach. Instead of computing the gradient at each datapoint every iteration, SDG updates the parameters by iterating through the dataset and using the gradient at each single datapoint. The dataset is then permuted and iterated through again until an approximate minimum is reached. Pseudocode of SDG is presented in algorithm 1.

Algorithm 1 Stochastic Gradient Descent (SDG)

```
Initialize parameters θ and learning rate γ
while Not converged do
    Permute training set (X, Y)
    for i in 1, ..., N do
        θ ← θ − γ∇_θ L(f_θ(x_i), y_i)
    end for
end while
```

TODO: Mini batch SDG

For the actual gradient computations, the backpropagation algorithm is used. It provides an efficient way of computing gradients in neural networks by leveraging the compositional structure. In essence backpropagation is an efficient application of the Leibniz chain rule for differentiation.

For a through introduction to the subject of neural networks and the training thereof we refer to chapter 6 and 8 of [5].

2.5 Convolutional Neural Network

This section draw inspiration on the presentation of convolutional networks in chapter 9 of [5].

A convolutional neural network (CNN) is a particular type of neural network that is developed to learn local features in the data. This local feature learning is enabled by the mathematical operation of convolution. In essence a CNN is a neural network where matrix multiplication is switched for convolution at least one of the layers [5].
Fully connected neural networks have a fundamental drawback in that their computational complexity grows intractably large when the input dimensionality is high. This makes them unsuited for high dimensional data, such as images. Convolutional neural networks directly address this issue via various downsampling techniques. Convolutional neural networks has a rich history and a long track record of success stories. They are inspired by the architecture of visual cortex cells in mammals. Inspired by the discovery of Hubel and Wiesel [6] the neocognitron was proposed in 1980[7]. The neocognitron is widely considered the predecessor of convolutional neural networks. In 1989 Yann LeCun et al. introduced the modern framework for CNNs [8] and demonstrated its effectiveness on the task of hand written digit recognition. Since then CNNs have been an indispensable part of machine learning research, especially in the computer vision domain. For an exposition on the advances on convolutional neural networks and its applications we refer to [9].

2.5.1 The convolution operation

The convolution operation is an integral transform with extensive applications. It generalizes the notion of a moving weighted average. In mathematics it is ubiquitous because of its relationship with the Fourier transform.

Let f and g be real valued functions, then their convolution is defined as

$$(f * g)(t) = \int_{-\infty}^{\infty} f(\tau)g(t-\tau)d\tau \tag{2.5}$$

The mathematical nuances of the exact criteria for the above integral to exist is outside the scope of this thesis, and not particularly relevant. But if f and g are integrable (in the Riemann or Lebesgue sense) then the convolution exists. As a rule of thumb, the convolution of f and g is as "smooth" as the smoothest of f and g. It is worth mentioning that convolution is commutative, i.e that $f * g = g * f$, which can be seen by a simple change of variables.

As is typical for integral transforms, the function g is referred to as the *kernel*. In the context of convolutional networks the kernel consists of learnable parameters and the function f is the *input*. The output is referred to as the *feature map* [5]. In machine learning we handle discrete signals, represented as multidimensional arrays. As a result we must employ a discrete variation of the convolution operation. Let I be the input and K be the kernel, both discrete, then their convolution is defined as

$$(I * K)[n] = \sum_{m=-\infty}^{\infty} I[m]K[n-m]. \tag{2.6}$$

In practice I and K typically has finite support, i.e they are zero for large positive and negative arguments, which circumvents any convergence problem.
Convolutions are naturally defined for higher dimensional functions by component wise extension. For a two dimensional image I and a kernel K we calculate their convolution as

$$(I * K)[i,j] = \sum_{n=-\infty}^{\infty} \sum_{m=-\infty}^{\infty} I[n,m]K[i-n, j-m]. \tag{2.7}$$

The operation is illustrated in figure **??**.

Convolution in machine learning does not always correspond exactly to the mathematical definition of the operation, but rather to cross-correlation. The difference is just a sign flip in the kernel arguments. Operation is no longer commutative, but in practice this does not affect anything as the learned kernel parameters will be equivalent [5].

In the field of digital signal processing discrete convolutions are used extensively. Traditionally predefined kernels are used to alter a signal in predictable ways. Two well known kernels are Gaussian and edge detection kernels. Gaussian kernels are two dimensional gaussian distributions and are used for blurring. Edge detection kernels are designed in such a way that areas of similar intensity are mapped to 0 and areas of variable intensity are mapped to high values. In figure 2.3 we demonstrate the effect of two such kernels. Edge detection in particular provide a hint to how CNNs learn interesting features in the data. In a convolutional layer the kernels are learned such that the feature map is helpful for the training objective.

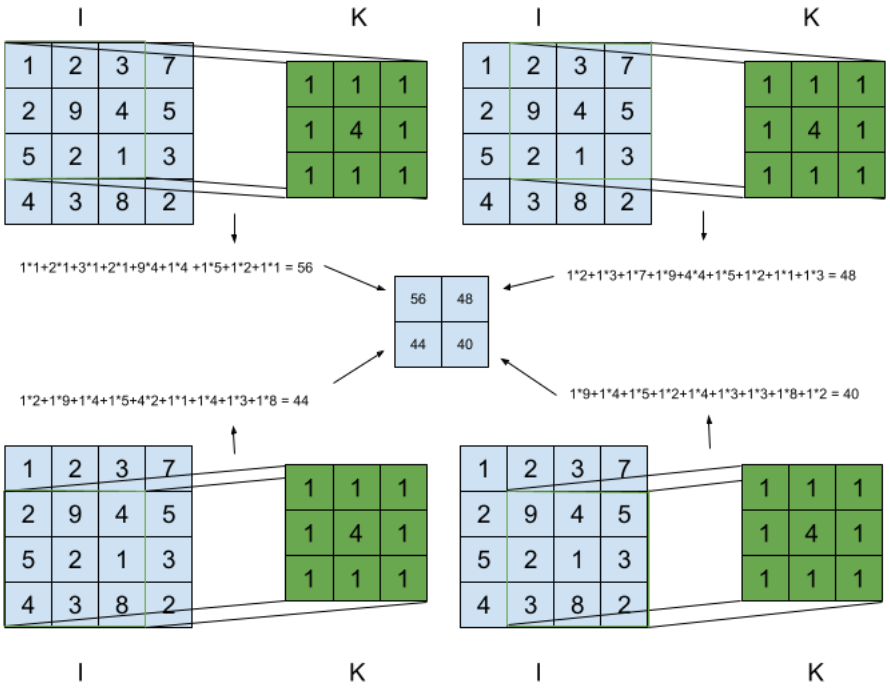

Figure 2.2: Illustration of discrete two dimensional convolution

2.5.2 Pooling

As mentioned earlier CNNs are mainly used when the data has high dimensionality. In order to reduce the dimension to a manageable level *pooling* is used. A pooling operation is applied as a down sample technique on feature maps, replacing regions of the output with summary statistics. Two of the most common are max and average pooling, which replaces the region by its maximal or average value respectively. There are two hyperparameters for any pooling operation, the filter size, which determines the region of values to calculate the summary statistic, and stride length, which determines how the filter moves across the feature map. In addition to dimension reduction, pooling assist in making the representations approximately invariant to small distortions of input. Illustrations of max pooling with different stride is presented in figure **??** and **??**, while the effect of max and average pooling on image data is illustrated in **??**.

2.5.3 Architecture

There are a large variety of specific architectures which fall in the category of a CNN, but their basic components are largely the same. They consist of convolutional layers, pooling layers and fully connected layers. In figure 2.8 an illustation of the original LeNet-5 [8] is presented as an illustration of a general CNN.

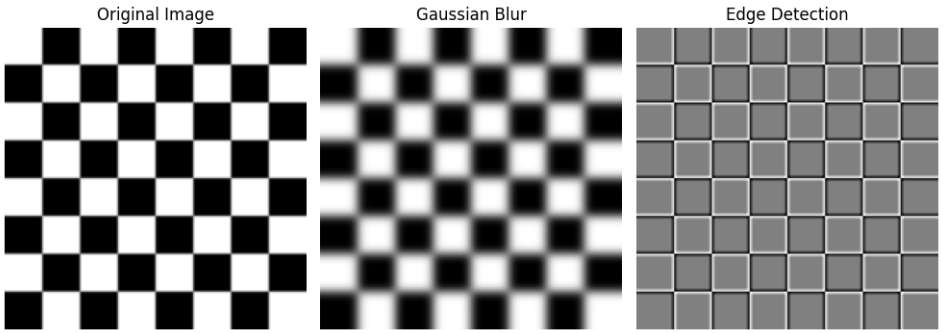

Figure 2.3: Illustration of discrete convolution applied to images. Image part of Scikit-image data package.

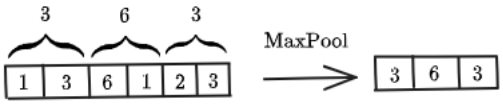

Figure 2.4: Max pooling of one dimensional array. Filter size: 2, stride: 2.

A convolutional layer consists of several kernels used to compute different *feature maps*. Each kernel convolved with entire input, and the different feature maps are produced by changing kernel. A nonlinear activation function is then applied pointwise to the feature maps. A pooling layer is typically placed between convolutional layers and work as a stronger downsampler which aims to enforce approximate translation invariance. A pooling operation is applied across each feature map.

The fully connected layer is just your typical hidden layer in a neural network, i.e connect every input to every node in the output. Because of computational issues mentioned earlier fully connected layers are first introduced when the input data has been sufficiently downsampled.

2.5.4 Transposed Convolutional Networks

Transposed convolution or deconvolution, also known as fractionally-strided convolution is a technique used to reverse the downsampling from convolutions. In essence it is an inpainting or upsampling technique known from digital signal processing. The flexibility of learning data dependent transposed convolutional kernels enables one to more effectively reverse the downsampling from convolutional layers. They are extensively used in combination with convolutional downsampling in *encoder-decoder architectures* presented in section 2.9.

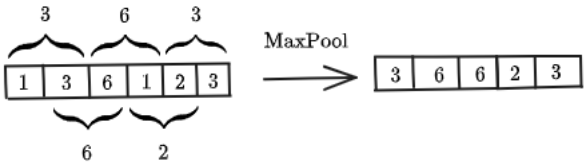

Figure 2.5: Max pooling of one dimensional array. Filter size: 2, stride: 1.

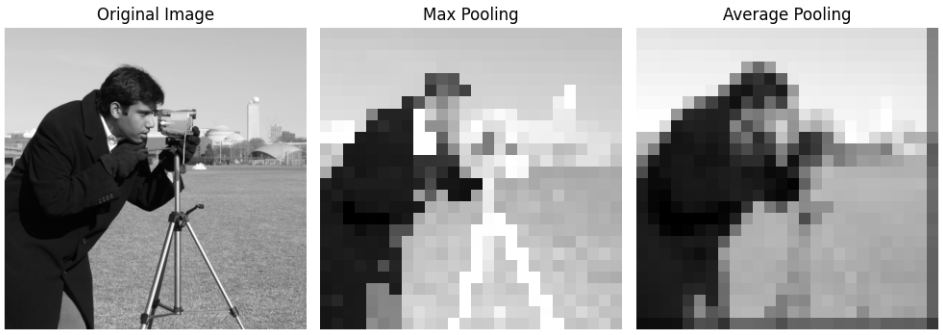

Figure 2.6: Illustration of mean and average pooling applied to images. Filter size and stride is 20×20. Original image size is 512×512, pooled images are 26×26. Image part of Scikit-image data package.

2.6 Representation Learning

The focus of this thesis is representation learning for improved time series generation.

2.6.1 Why do we care about representation learning?

Those who has worked with data science or machine learning and has come across feature engineering are familiar the effect good feature engineering has on a models performance. The same people too knows the level of domain expertise, creativity and time is needed to feature engineer well. In reality much of the actual time spent in the process of deploying machine learning methods revolves around constructing good data pipelines and applying transformations that produce representations beneficial for the algorithm at hand [10]. Thus the ability to automate such tasks would be incredibly beneficial, and ease the use of ML algorithms significantly. It is here one of the intriguing and promising features of neural networks, with its many specializations and architectures, comes into play. They have shown the ability to learn useful abstract representations of the data and provide automatic feature engineering [10].

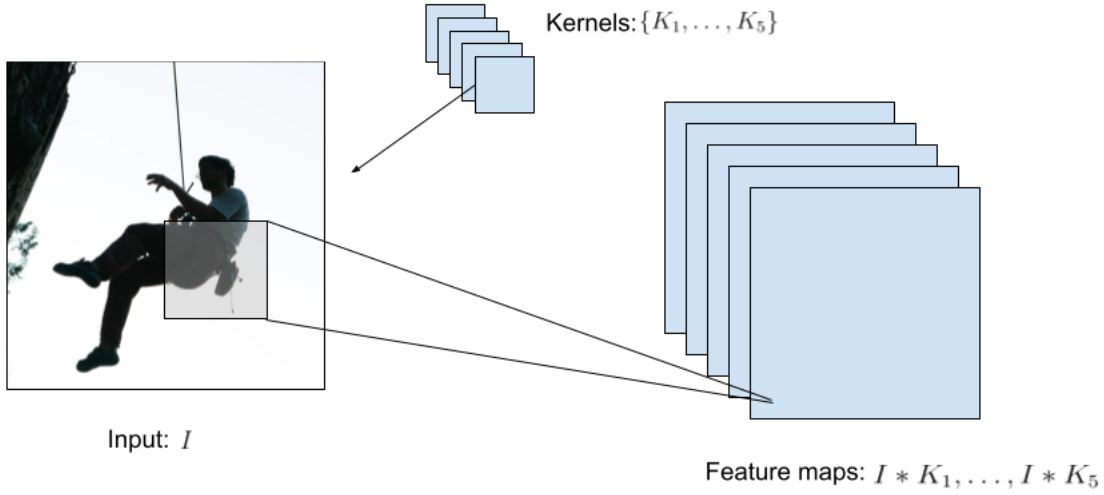

Figure 2.7: Convolutional layer.

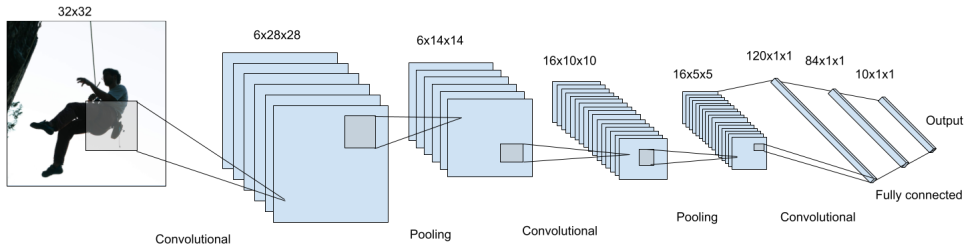

Figure 2.8: LeNet-5 network [8]

2.6.2 What a representation?

Representation learning is a term not too easily defined, one reason being the abstraction level. It is helpful to first consider what is meant by *representation* of information. Lets begin by walking through a familiar and illustrative example. Consider the base ten integer $(4)_{10} = 4$. The number can equivalently (in terms of information content) be expressed, that is represented, in any other base. The particular base we choose depends on our intention with the number. If we want to work with digital electronics, a binary representation ($(4)_2 = 10$) is very useful, as transistors has two states. When humans do arithmetic, base ten representations of the integers are very natural, as we have ten fingers. A particular representation of information can make a task easier or harder. The information content is unchanged by a change of representation. What is changed is the easiness or difficulty of certain information processing tasks. Representation learning is then the process of learning a certain representation of information.
Representations are too highly dependent on who, or what, that will process it. An example is time. Humans have developed a standardized system for writing

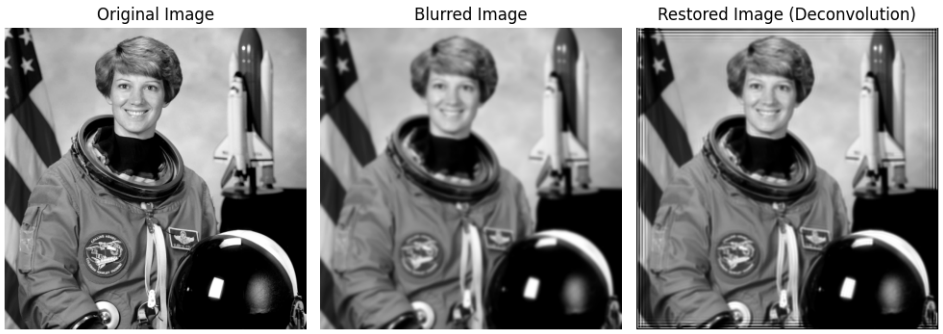

Figure 2.9: Illustration of deconvolution applied to images. Here using Gaussian blur and restoring using the Richardson Lucy algorithm with a Gaussian deconvolution kernel. Image part of Scikit-image data package.

timestamps which works fairly well for us. But, if we want to model time dependent phenomena, say using tabular data, the DateTime representation is of very little help to a tree based model for instance. The reason being that the numerical representation of timestamps close in time is not necessarily close in numerical value. Think of 23:59 to 00:00. A possible solution is to change the representation such that the numerical values actually respect the periodic nature by mapping to the circle. The new representation is then useless for humans, but quite a lot more useful to a computer. Representation learning in machine learning can thus be thought of as algorithms which are designed to learn representations which is useful for a ML objective.

2.6.3 What is a good representation?

The goodness of a representation is then determined by how easy it makes a subsequent task. The concept of universally good representations is ill-defined, for any representation extracted of a non-invertible function, a *downstream tasks* can be designed (in principle) to based on the lost information, hence achieve arbitrarily bad performance. There is no free lunch in representation learning either. One must specify a set of predefined downstream tasks, and evaluate according to those. Intuitively the quality of the representations are also considered higher if the the representations is able to perform well on several downstream tasks i.e when they are more general.

2.6.4 How does one evaluate representations?

There are several different evaluation protocols in representation learning. They involve training a model on a *pretext task*, which as defined in [11] is a task for a network to solve, where the goal is to learn representation. Then the learned representations are evaluated on a downstream task. In general the downstream task is solved in a supervised manner, using human annotated data.

In a N-layered network $f = f_N \circ ... \circ f_1$, the intermediate value of the data x in some layer n is what is meant by the networks learned feature representations. When we are interested in the representations learned it thus is helpful to dissect a model f, notation wise, into a *feature extractor* h and an *output function* g such that it can be factored as $f = g \circ h$. Representation learning algorithms typically follow the pattern

- Train $f = g \circ h$ on a pretext task.
- Discard g
- Use the learned feature extractor $\widehat{h}$ as part of a new model.
- Evaluate the new model on the downstream task.

The standard evaluation protocol is to train a linear head g_D on top of the *frozen* representations in a supervised manner and evaluate this models performance. This is to say that we train $f_D = g_D \circ \widehat{h}$ by only updating the parameters of the linear model g_D, and evaluate $\widehat{f_D}$ on some test set. This protocol is sometimes referred to as *linear probing*. A common downstream task is classification, where the idea is that good and informative representations should differentiate data in such a way that it is easy to separate them.

An common alternative protocol is similar to the one above, but rather than freezing the feature extractor one let all parameters of f_D to be learnable on the downstream task. This protocol is referred to as a pretraining-finetuning.

It is of interest how f_D performs in terms of accuracy on the downstream task and training time, and too how these sensitive metrics are to training data size. The baseline comparison would then be an identical but randomly initialized model. It is considered highly advantageous if one is able to pretrain a feature extractor using cheap and abundant data in a way which ensures faster convergence on a downstream task where data is expensive or scarce.

It is with mentioning that in cases where the sole goal is to create the best performing model, a more complex task specific head g_D is often used. For a comprehensive survey on representation learning we refer the reader to [12].

2.7 Transformers

Since their introduction in the seminal paper titled "Attention is all you need"[13] transformers have taken the field of machine learning and artificial intelligence by storm. It is the enabling architecture behind large language models (LLMs) such as Googles BERT, Metas Llama and OpenAIs ChatGPT. Drawing inspiration from the initial success in natural language processing vision transformers [14] were developed for computer vision applications, and similar trends are shown for other modalities such as audio [15] and time series [16].

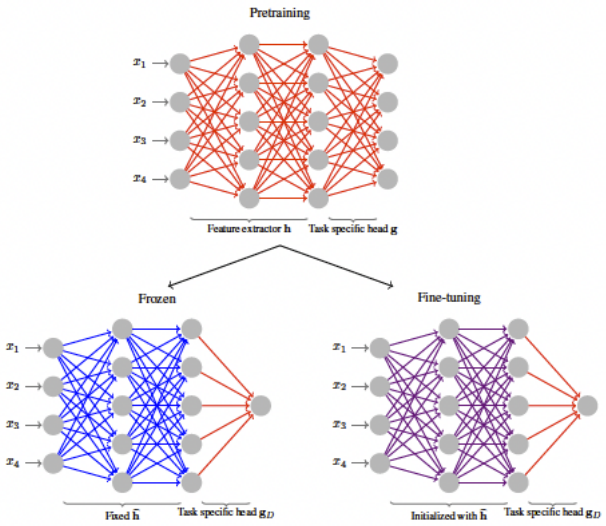

Figure 2.10: Taken from [12]

Transformers were developed for sequential modelling and has capabilities of learning far ranging dependencies in data through the *multi-headed attention mechanism*. In the realm of sequential modelling recurrent neural networks and long short-term memory neural networks were the previous state of the art, but modeling long term dependencies has proven difficult [17] as one encounters the *vanishing or exploding gradient problem*. One of the main novelties of the transformer architecture is not relying on recurrence, and instead solely using the attention mechanism to capture dependencies between input and output.

cite

cite

The transformer takes as input a sequence of symbols , referred to as the *input embedding* in **??**. This means in particular that for a specified modality, e.g text, speech, image and time series, they must first be translated into a sequence of vectors. This is accomplished by a process called *tokenization*. The conceptually easiest word-level tokenization in NLP, where one creates a dictionary of all words in the dataset, and assigns to them an integer value. A piece of text can then with relative ease be mapped to a sequence of integers. Other modalities as speech, image and time series are usually represented as matrices and can therefore naively be modeled as a sequence numbers. Because of the high dimensionality, this would require a significant amount of computational resources. In addition the transformer would need to model incredibly far ranging dependencies and handle redundant information. Hence various tokenization methods are used to represent the data as coarser sequences.

Transformers can be adopted for generative tasks, and has done so with great

success. Autoregressive transformers such as the GPT series are trained to predict the next token in a sequence given the preceding tokens. By treating images as sequences of patches vision transformers can generate new images or inpaint missing patches conditional on the input. With the introduction if vision transformers [14], input images were split into patches and linearly projected before being processed by the transformer. Since then *Vector-Quantized*-based tokenization introduced by [18] has emerged as a popular approach.

2.7.1 The attention mechanism

"Attention can be described as mapping a query and a set of key-value pairs to an output, where the query, keys, values and outputs are all vectors".

TODO: Wait for 3b1b video for context

Scaled dot-product attention,

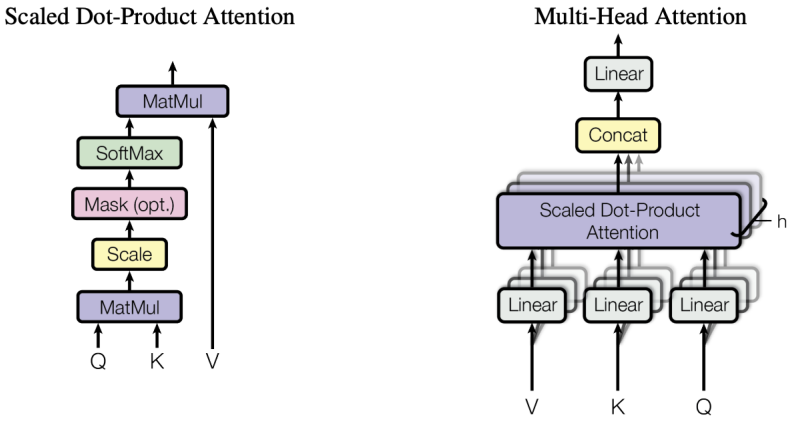

Figure 2.11: (left) Scaled dot-product attention. (right) Multi-headed attention. Taken with permission from [13]

$$\text{Attention}(Q,K,V) = \text{SoftMax}\left(\frac{QK^T}{\sqrt{d_k}}\right)V \tag{2.8}$$

Multi-headed attention

$$\text{MultiHead}(Q,K,V) = \text{Concat}(\text{head}_1,\ldots,\text{head}_h)W^O \tag{2.9}$$

where

$$\text{head}_i = \text{Attention}(QW_i^Q, KW_i^K, VW_i^V) \tag{2.10}$$

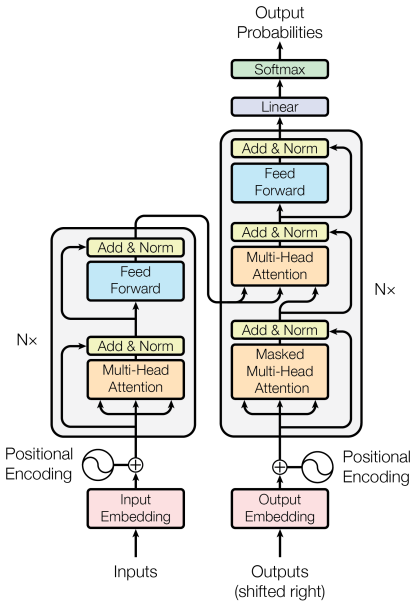

Figure 2.12: The Transformer - model architecture. Encoder (left), decoder (right). Taken with permission from [13]

2.7.2 Architecture

Encoder - decoder architecture.

Tokenizer

Positional encoding

Transformer layer (encoder/decoder)

2.7.3 Bi-directional transformer (BERT)

Encoder only transformer. Unidirectional

2.8 Self-Supervised learning

Self-supervised learning (SSL) has had great success in natural language processing and computer vision in recent years.

Machine learning can be coarsely divided into two classes, supervised and unsupervised learning.

2.8.1 Supervised

Supervised learning refers to models who learn using labeled data. That is to say for a given input x we already know what the desired output y is during training, and can therefore supervise (update) our models parameters by directly comparing model output and the true value. A bit more formally, for a dataset $X =$

$\{x_i\}_{i=1}^N$ with corresponding human annotated labels $Y = \{y_i\}_{i=1}^N$, the objective of a supervised learning algorithm is to fit f_θ in such a way that the loss across the data is minimized

$$\widehat{f}_\theta = \min_\theta \frac{1}{N} \sum_{i=1}^{N} L(f_\theta(x_i), y_i). \tag{2.11}$$

Common approaches to supervised learning for neural networks is to calculate some distance metric between the predicted value $\widehat{y}$ and the true value y and update parameters by backpropagation.

The models falling under the supervised learning category are widely deployed and has seen tremendous success. Classical statistical models, as well as support vector machines and decision tree based models are all examples of models in this learning paradigm. The main issue with supervised learning is the need for labeled data, and labeled data is in many ways scarce.

2.8.2 Unsupervised

Unsupervised learning on the other hand refers to models or algorithms who learn exclusively from unlabeled data. That is to say that the models learn intrinsic patterns in the data. Examples of unsupervised learning models are clustering methods as K-means, K Nearest Neighbor and Gaussian mixture models, dimension reduction techniques as PCA/SVD and neural network architectures such as Autoencoders.

TODO: Where is it used an why?

Exploratory data analysis, data visualization, clustering

TODO: Pros and cons of unsupervised learning

Unlabeled data is cheap,

2.8.3 Self-supervised

Self-supervised learning is subcategory of unsupervised learning and refers to model who use the data itself to generate a supervisory signal, rather than external labels as in supervised learning. Even as SSL is considered unsupervised learning, the learning formulation is quite similar to that of supervised learning.

For a dataset $X = \{x_i\}_{i=1}^N$ with *pseudo labels* $P = \{p_i\}_{i=1}^N$ the objective of a self-supervised learning algorithm is to fit f_θ in such a way that the loss across the data is minimized. In other words find

$$\widehat{f}_\theta = \min_\theta \frac{1}{N} \sum_{i=1}^{N} L(f_\theta(x_i), p_i). \tag{2.12}$$

A pseudo label is an automatically generated label from the data attributes in the pretext task. In joint embedding architectures the pseudo labels are typically

some *augmentation* of the original data.

SSL has in recent times (since 2018??) been a fruitful approach to unsupervised representation learning and has played an integral part in the boom of large language models together with the invention of the transformer architecture. With models growing ever larger and more data hungry SSL is essential in pretraining. Randomly initialized networks are difficult to train and requires a lot of time and computational resources. SSL has shown remarkable results when used for pretraining. That is as models for learning network parameters who capture semantics of data, without the need for labels. Pretraining networks enables foundation models, which can be trained for many different tasks in a supervised fashion requiring a lot less resources.

In recent years, especially in computer vision and natural language applications, SSL methods have shown incredible promise in representation learning. SSL methods have proven close to, and sometimes surpassing, supervised methods on downstream tasks. This has inspired researchers to apply SSL methods across other modalities.

TODO: Find sources backing this up.

TODO: What are the different flavours of SSL?

Generative: Masked modelling Discriminative: Contrastive/non-contrastive Autoassociative: Autoencoder type - Essentially try to make composition the identity despite a compression. Usually not considered SSL, but it technically is.

TODO: What are some of the issues?

Siamese Architecture-based SSL

[19] A siamese network architecture [20] consists of two networks, called branches, with a shared encoder on each branch. Such networks are trained to produce similar representations for different views of the same data.

In models with such architecture, the existence of trivial solutions, such as both networks ignoring input and produce identical constant embeddings, is a major issue. This issue is referred to as *collapse* of the model.

Augmentations for creating different views. The role of augmentations, types etc. Augmentations across modalities. [21]

In the computer vision domain several representation learning algorithms utilizing a siamese architecture have been proposed. They mainly fall under two categories: *contrastive* and *non-contrastive* methods.

In contrastive SSL, uses positive and negative samples and learns representations by pulling positive pairs closer together and negative pairs further apart. Examples include MoCo [22] and SimCLR [23]. SimCLR constructs two correlated samples by applying augmentations to an input sample, and considers these as positive pairs. Requires large batch sizes in order to work well.

Need large number of negative pairs compared to positive in order to learn representations effectively [19].

The loss function of contrastive SSL attempts to minimize the distance of positive sample pairs (+,+) and (-,-), and maximize the distance between negative sample pairs (+,-) and (-,+).

Non-Contrastive: Collapse, where encodes produce uninformative or constant vectors. The different ways of handling collapse. How Variance-Covariance regularization (VCReg) [24] has emerged as a minimal(??) solution.

TODO: Talk about projectors in ncSSL. How and why they enforce pairwise independence

BYOL, Barlow Twins, VCReg, VICReg, VIbCReg
[24] VCReg for pairwise independence in SSL representations.

2.8.4 Masked modelling

Masked modelling is a conceptually simple self-supervised learning technique for generative models. The idea is to mask or cover a portion of the data and predict the masked portions. By comparing the prediction against unmasked data the model can learn useful representations without supervision. Since the introduction of masked modelling in natural language processing by [25] it has been the de-facto standard for self-supervised pretraining of language models. BERT introduced masked modeling for language representation learning as means to use bi-directional transformers without enabling each word to "see itself".

TODO: When did GPT [26] use Masked modelling?

Masked image modelling [27]: Mask image patched directly
When vision transformers [14] surpassed CNN in 2021[28], CV research began to draw inspiration more heavily from [25] and began tokenizing images and pretraining transformers.
Masked visual token modelling [29]: Tokenize the image and mask tokens.

TODO: Masking in original domain or tokens. Masking strategies.

For a thorough survey on masked modelling for SSL in the vision domain we refer to [30].

2.9 Vector Quantized Variational Autoencoder (VQVAE)

Our model is based on the Vector Quantized Variational Autoencoder (VQVAE) introduced in [18], and includes an Auto-encoder (AE) branch. Therefore it is natural to dive into the models. We first start with introducing auto-encoders, then present the variational variation VAE before presenting VQVAE.

2.9.1 Autoencoder (AE)

Consists of two neural networks, an encoder E and decoder D. They can be seen as maps between spaces X and Z, where we refer to X as the data space and Z as the latent space.

$$X \xrightarrow{E} Z \xrightarrow{D} X \tag{2.13}$$

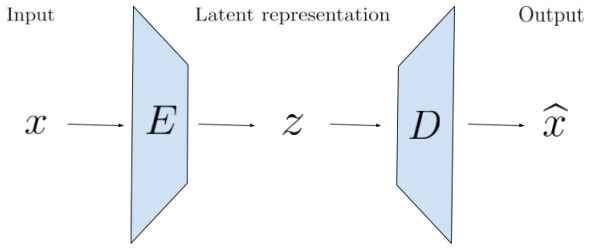

Figure 2.13: Schematics of the autoencoder architecture.

The autoencoder is trained in such a way that the composition of encoder and decoder is approximate to the identity. Typically the dimension of the latent space is much lower that that of the data space. Encoder and decoder then compresses and decompresses the data and learns efficient *latent representations*.

TODO: Information bottleneck

TODO: Issues with latent representations and the need for regularization

2.9.2 Variational Autoencoder (VAE)

Variational Autoencoders (VAE) were introduced in [31] and is a variational Bayes approach to approximate inference and learning with directed probabilistic models. The architecture of VAE is similar to AE, but the mathematical formulation is quite different. For context variational inference is a technique in statistics used to approximate complex distributions by looking for the closest approximation within a simple, but flexible, parametric family.

In the VAE framework we assume that the dataset $X = \{x_i\}_{i=1}^N$ consists of iid samples from a random variable $\mathbf{x}$. We further assume that the data is generated by some unobservable random process. This is to say that we assume there is a random variable $\mathbf{z}$ such that $x_i \sim p_{\theta^*}(x|z_i)$, where $z_i \sim p_{\theta^*}(z)$. The distribution

$p_{\theta^*}(z)$ is referred to at the true prior and $p_{\theta^*}(x|z_i)$ as the true likelihood. As **z** is unobservable and the true distributions are unknown, one has to assume their form. In general the prior and likelihood are assumed to be from parametric families $p_\theta(z)$ and $p_\theta(x|z)$. As with any model where one wishes to employ gradient based learning, the distributions are assumed to be differentiable almost everywhere, both with respect to their parameters and argument.

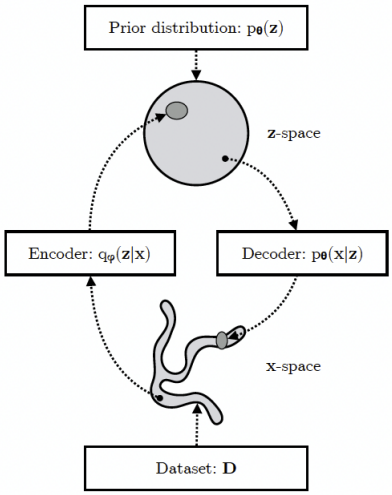

Figure 2.14: [32], need to ask for permission or make own

VAEs have two components to their architecture. The first is a probabilistic encoder, often called the inference model, $q_\phi(z|x)$ which approximates the true posterior. Secondly a probabilistic decoder, often called the generative model $p_\theta(x|z)$, which approximates the likelihood. These models are typically parameterized by some type of neural network, and in that case ϕ and θ are the weights and biases of the two networks. Given a datapoint x_i the probabilistic encoder provides a distribution over the possible values of the latent variable **z**. Similarly, given a latent representation z_i the probabilistic decoder produces a distribution over the possible corresponding values of **x**.

The probabilistic part of the encoder and decoder is the sampling. The output for a given x or z is a distribution, and for the same input the same output distribution is calculated (as long as the network parameters are frozen). Actually x and z are mapped to the parameters of a distribution, which uniquely determines the distribution in a particular family.

The most common situation is to assume

- Prior $p_\theta(z) \sim N(0, I)$
- Likelihood $p_\theta(x|z) \sim N(D(z), I)$

- Variational posterior $q_\phi(z|x) \sim N(E(x)) = N(\mu_x, \Sigma_x)$

The encoder maps datapoints to parameters of the variational distribution, i.e the approximate posterior q_ϕ, $x \mapsto E(x) = (\mu_x, \Sigma_x)$. A latent representation z is then sampled from q_ϕ, which constitutes the random part of the algorithm. The decoder maps z to the expected value of the likelihood $p(x|z)$, $z_i \mapsto D(z_i)$.

There are several reasons for choosing Gaussian distributions, one being that the Gaussian distribution a scale-location family. This enables us to circumvent the problematic random component in the VAE when using gradient based learning. As described above we sample $z \sim N(\mu_x, \Sigma_x)$ where $E(x) = (\mu_x, \Sigma_x)$. We can equivalently sample from $N(\mu_x, \Sigma_x)$ by reparameterization using the location-scale property. This means to introduce an auxillary variable $\epsilon \sim N(0, I)$ and rewriting $z = \mu_x + L_x\epsilon$, where L_x is the Cholesky decomposition of Σ_x. This factors the random part out of path of gradient flow.

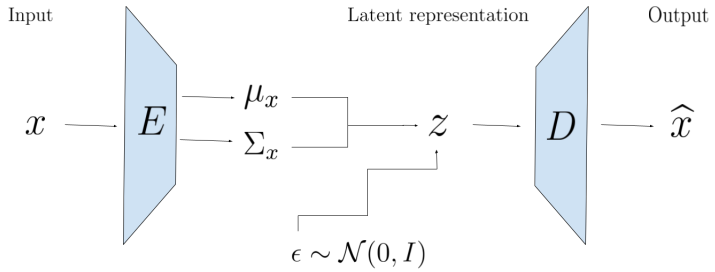

Figure 2.15: Schematics of the VAE architecture with Gaussian reparameterization.

Training objective

As with other variational methods VAEs are optimized with respect to the *evidence lower bound* or ELBO for short. Let **x** and **z** be two jointly distributed variables, with distribution p_θ. Then for any distribution q_ϕ the ELBO is defined as

$$\mathcal{L}_{\theta,\phi}(x) = \mathbb{E}_{q_\phi(z|x)} \log\left(\frac{p_\theta(x,z)}{q_\phi(z|x)}\right) \tag{2.14}$$

The ELBO can be reformulated in terms of the marginal likelihood and KL divergence of the variational to the true posterior.

$$\begin{aligned}\mathcal{L}_{\theta,\phi}(x) &= \mathbb{E}_{q_\phi(z|x)} \log(p_\theta(x)) + \mathbb{E}_{q_\phi(z|x)} \log\left(\frac{p_\theta(z|x)}{q_\phi(z|x)}\right) \\ &= \log(p_\theta(x)) - \mathrm{KL}(q_\phi(z|x)||p_\theta(z|x)).\end{aligned} \tag{2.15}$$

Due to the non-negativity of the KL-divergence, we see that the ELBO bounds the marginal log likelihood of the data from below. By maximizing the ELBO with

respect to the model parameters ϕ and θ one simultaneously maximizes the marginal likelihood, which improves the generative model, as well as reducing the KL-divergence of the approximate to the true posterior, which improves the inference model [32].
An alternative reformulation gives a more evident connection to Autoencoders, with a the prior acting as a regularizer on the posterior

$$\begin{aligned}\mathcal{L}_{\theta,\phi}(x) &= \mathbb{E}_{q_\phi(z|x)} \log\left(p_\theta(x|z)\right) - \mathbb{E}_{q_\phi(z|x)} \log\left(\frac{q_\theta(z|x)}{p_\phi(z)}\right) \\ &= \underbrace{\mathbb{E}_{q_\phi(z|x)} \log\left(p_\theta(x|z)\right)}_{\text{Expected reconstruction log likelihood}} \underbrace{- \mathrm{KL}(q_\phi(z|x)||p_\theta(z))}_{\text{Regularizer}}.\end{aligned} \tag{2.16}$$

As the $p_\theta(x|z)$ is typically assumed to be Gaussian we have

$$\log p_\theta(x|z) = -\frac{1}{2}\left[k\log(2\pi) + (x - D(z))^T(x - D(z))\right], \tag{2.17}$$

which is equivalent, as an optimization objective of $D(z)$, to $||x - D(z)||_2^2$. Consequently the likelihood in the loss is implemented as the MSE of the input x and the output $D(z)$.

Generative model

The role of the prior in a VAE is two fold. Firstly as a regularizing constraint for the posterior during training, and secondly as a way of obtaining new samples x via ancestral sampling. Ancestral sampling refers to $\mathbf{z}$ being the parent node of $\mathbf{x}$ in the VAE, and that we can generate samples x by drawing a sample $z \sim p(z)$ and decode $D(z)$.

TODO: Speak on limitations of VAE before introducing VQVAE

Variational autoencoders has the issue of collapsing. Variance issues.

2.9.3 Vector Quantization (VQ)

Dictionary learning model [33]

2.9.4 VQVAE

The Vector Quantized Variational AutoEncoder (VQVAE) was first introduced in [18] and presented a new way of training VAEs with discrete latent variables. It is the first discrete VAE model which has similar performance to the continuous variant. VQVAE was developed to learn useful discrete representations for generation. This is enforced by more flexible distributional assumptions, as they say "Our model, the Vector Quantised- Variational AutoEncoder (VQ-VAE), differs from VAEs in two key ways: the encoder network outputs discrete, rather than continuous, codes; and the prior is learnt rather than static."-[18].

The overall architecture of VQVAE consists of an encoder and decoder as before, together with a *codebook* which is used in the quantization process. The codebook, also referred to as the latent embedding space, $\mathcal{Z} = \{z_k\}_{i=1}^{K}$ is consists of K latent vectors with dimensionality D. It can be considered a lookup table of vectors that are used for vector quantization (VQ). The output of the encoder $E(x)$ is quantized by the means of nearest neighbor lookup

$$z_q = \arg\min_{z_k \in \mathcal{Z}} ||E(x) - z_k||. \tag{2.18}$$

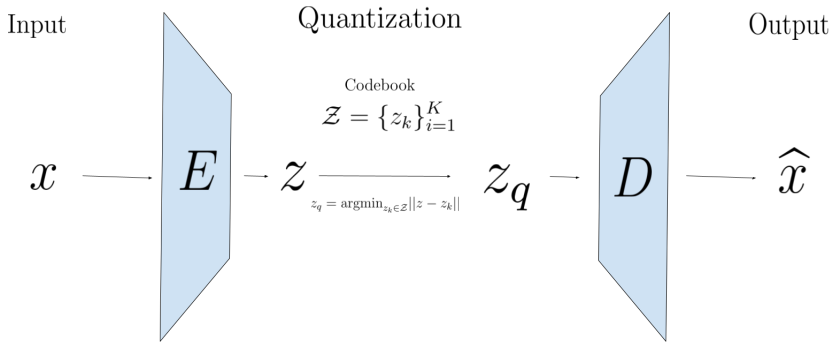

Figure 2.16: Schematics of the VQVAE architecture.

From 2.16 we can see that the VQVAE can be seen as an autoencoder with a nonlinearity introduced by the vector quantization.

In the original article [18] they propose to separately learn the prior distribution, after the encoder, decoder and codebook is learned. During the initial training the prior is assumed to be uniform, which poses no constraint on the posterior learning.

In contrast to VAEs the posterior is assumed to be categorical, as opposed to normal and the probabilities are defined as

$$p(z = k|x) = \begin{cases} 1 & \text{for } k = \arg\min_j ||E(x) - z_j||_2 \\ 0 & \text{otherwise} \end{cases}, \tag{2.19}$$

Sampling from the posterior amounts to quantizing the output of the encoder, as it is deterministic.

VQVAE can be viewed as a VAE, hence we can bound the marginal likelihood with the ELBO 2.16. As the variational posterior is deterministic and the prior (during training) is uniform over $\{1, ..., K\}$ we get that the regularizing term

$$\begin{aligned}
\mathrm{KL}(q(z|x)||p(z)) &= \sum_z q(z|x) \log\left(\frac{q(z|x)}{p(z)}\right) \\
&= q(z=k|x) \log\left(\frac{q(z=k|x)}{p(z=k)}\right), \; q \text{ is deterministic} \\
&= \log\left(\frac{1}{1/K}\right), \text{ uniform prior} \\
&= \log(K),
\end{aligned} \tag{2.20}$$

is constant. Consequently the ELBO reduces to the reconstruction term only.

TODO: Can think of the codes as the modes of a mixture of Gaussians, and instead of sampling from the mixtrure you just choose the closest mode.

Prior Learning

During the initial training the prior is as mentioned constant and uniform such that the posterior has more flexibility. After training an autoregressive prior is fit on z so we can sample x via ancestral sampling. The prior is learned with a generative objective, which increases the quality of generated samples. The choice of prior model depends on the particular application and in VQVAE PixelCNN [34] was used for image, while WaveNet [35] was used for audio. More recently in TimeVQVAE [1] utilized a bidirectional transformer [29] for prior learning in the time series domain.

Loss funciton

As we want to do gradient based learning, and the quantization process is quite far off from being continuous, measures has to be taken. The output of the encoder and the input of the decoder has the same dimension, which opens the possibility of simply copying the gradients from the decoder input to the decoder output. This is referred to as the *straight through estimator*. The gradients from the decoder contains relevant information to how the encoder should change its output, and in the subsequent forward pass the encoder output can be quantized to different discrete latent codes.

The loss function consists of three parts, the reconstruction loss, VQ loss and commitment loss. We already mentioned that the ELBO objective reduced to the reconstruction term only. In order to learn the codebook one uses the VQ loss, which is the euclidean distance between the encoder output and the quantized output. The final part of the loss is the commitment loss, which is introduced to keep the distance between embedding vectors (or codes) from growing arbitrarily large. To summarize the total loss is given by

$$\begin{aligned} \mathcal{L}_{\text{Recon}} &= ||x - \widehat{x}||_2^2 \\ \mathcal{L}_{\text{VQ}} &= ||sg(z) - z_q||_2^2 + \beta||z - sg(z_q)||_2^2 \\ \mathcal{L}_{\text{VQ-VAE}} &= \mathcal{L}_{\text{VQ}} + \mathcal{L}_{\text{Recon}} \end{aligned} \tag{2.21}$$

where β is a tuning parameter typically set to be 0.25 and $sg()$ is the stop-gradient operation, defined to be the identity with zero partial derivatives.

To illustrate the need for commitment loss and what it does consider a model where the data is either 0 or 1 and we initialize the codebook with $\mathcal{Z} = \{-1, 1\}$. The range of the encoder is $\mathbb{R}$ and $E(x)$ is quantized to -1 if its negative and 1 if its positive. Assume that the encoder and decoder will try to differentiate between the two classes by pushing $E(0)$ and $E(1)$ away from each other. As the reconstruction loss only affects the encoder and decoder, and the VQ loss only affect the codebook, we get that when the encoder and decoder parameter trains faster than the codebook, then the distance between the encodings and the codewords will steadily increase and the VQ loss diverge. This behavior is observed experimentally.

2.10 Evaluation metrics

2.10.1 Tokenization model

The tokenization model, as we are interested in representation learning, is evaluated on two metrics. Firstly, and most importantly its ability to reconstruct the input data once compressed into latent space. In essence the latent representation encodes "everything" (important information is preserved) about the original data if the model is able to reconstruct well. Secondly we evaluate linear classifiers on the latent representations, which provides good results if the model learns discriminative features of the different classes and produces an approximately linear separable space. Finally, as the tokenization model is a part of the generative model, the ultimate evaluation metric is the corresponding evaluation of the generative model.

Reconstruction

Downstream Classification

SVM, KNN. The difference in inductive bias for the two classifiers.

2.10.2 Generative model

Good evaluation protocols for generative models are hard to come by, and the hunt for such is an active area of research. There are data modalities for which

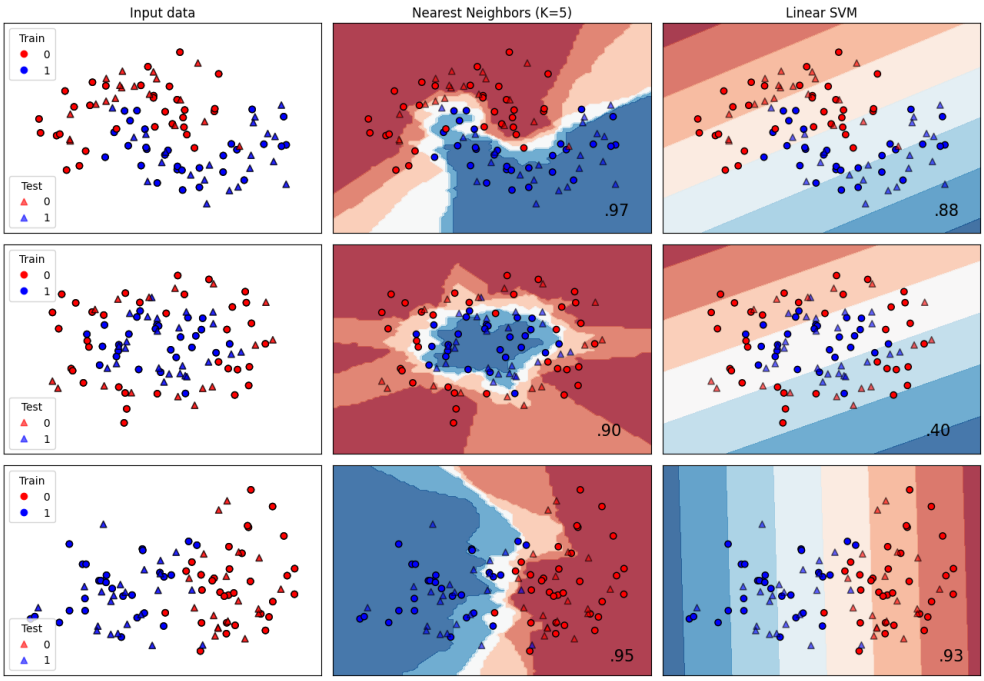

Figure 2.17: Modified example taken from `https://scikit-learn.org/stable/auto_examples/classification/plot_classifier_comparison.html`.

such evaluation metrics have more established standards than others. Most notably in the computer vision domain there is a benchmark dataset (ImageNet) and classifier (Inception v3).

The typical sanity check for generative models is human visual inspection. In development of evaluation metrics for generative models, how well a proposed metric correlates with quality determined by visual inspection is standard. Most people know what cats and dogs look like and can recognize features even in crudely generated images. In contrast, many time series dataset measure quantities and signals for which the untrained eye has no idea of determining the quality. This is one of the obstacles in TSG. Despite this, according to [1] the most common evaluation protocols in the TSG literature is PCA and t-SNE analyses on time series to visually see similarities of two distributions. The major limitations of this is that the visual inspections cannot be reduced to a single score, which makes objective comparison difficult.

Following [1] we mainly consider three evaluation metrics in this thesis. *Inception Score* (IS), *Fréchet Inception Distance* (FID) and *Classification Accuracy Score* (CAS). IS measures quality of synthetic samples using the entropy of the label distribution and the evenness in prediction across labels. The *Fréchet Inception Distance* measures a distance between the generative and ground truth distribu-

tion. Finally the *Classification Accuracy Score* measures the quality of the class-conditionally generated samples by training a classifier on synthetic data and testing on real.

Common for all the above evaluation metrics is the reliance on a pre-trained classification model. In contrast to computer vision there is no widely adopted classification model for time series, but in [36] a fully convolutional network (FCN) was presented as a proposed baseline classification model for time series. As their model is not available we use the open source FCN trained on the UCR Archive presented in [1] for our evaluations.

Inception Score (IS)

Inception Score (IS) was first introduced in [37] as an automatic evaluation method of synthetic samples.
The Inception Score works by applying a classifier to every generated sample to get the conditional label distribution $p(y|x)$. Samples containing clear characteristics should have low entropy, i.e one should be certain of the label. In addition we expect a good model to generate varied samples, so the marginal $\int p(y|x = D(z))dz$ should have high entropy. On this basis, the Inception Score is defined as

$$\mathrm{IS}(\theta) = \exp\left(\mathbb{E}(D_{\mathrm{KL}}(p_\theta(y|\mathbf{x})||p_\theta(y)))\right). \tag{2.22}$$

In contrast to computer vision there is no widely adopted classification model for Time Series. In [36] a fully convolutional network (FCN) was presented as a proposed baseline classification model, and we use the open source FCN trained on the UCR Archive presented in [1] for our evaluations.

Let $X_{\mathrm{gen}} = \{x_{i,\mathrm{gen}}\}_{i=1}^{N}$ be a set of generated samples. We use the apply a SoftMax layer to pretrained FCN representations to obtain an estimate of the conditional label distribution as follows

$$x_{i,\mathrm{gen}} \xrightarrow{\text{FCN+SoftMax}} p(y|x_{i,\mathrm{gen}}).$$

The marginal label distribution is obtained by averaging across all the synthetic data as follows

$$p(y) = \frac{1}{N}\sum_{i=1}^{N} p(y|x_{i,\mathrm{gen}}).$$

Issues with IS [38] (Use different network, for image classification). Important to report different metrics that indicate that the model has not overfitted. Also issues with IS [39].

Fréchet Inception Distance (FID)

As an attempt to improve on IS [40] introduced the Fréchet Inception Distance (FID). Since then FID has been the standard for assessing generative models [39]. The primary concern with IS is, as mentioned earlier, that it does not use any statistics of real world samples to compare with the statistics of the generated samples. In contrast FID relates the synthetic sample to the real world samle via the *Fréchet distance*. For any two probability distributions, f, g over $\mathbb{R}^n$, with finite mean and variances, their distance is defined as

$$\begin{aligned} d_F(f,g) &= \left(\inf_{\gamma \in \Gamma(f,g)} \int_{\mathbb{R}^n \times \mathbb{R}^n} ||x-y||_2^2 d\gamma(x,y) \right)^{\frac{1}{2}} \\ &= \left(\inf_{\gamma \in \Gamma(f,g)} \mathbb{E}_{(x,y)\sim\gamma} ||x-y||_2^2 \right)^{\frac{1}{2}}, \end{aligned} \tag{2.23}$$

where $\Gamma(f,g)$ is the set of all *couplings* of f and g. The Fréchet distance is a special case of the Wasserstein metric and will in literature be referred to as such.

In [41] it was shown that for two Gaussian distributions the Fréchet distance is explicitly solvable as

$$d(\mathcal{N}(\mu,\Sigma),\mathcal{N}(\mu',\Sigma'))^2 = ||\mu-\mu'||_2^2 + \mathrm{Tr}\left(\Sigma+\Sigma'-2(\Sigma\Sigma')^{\frac{1}{2}}\right) \tag{2.24}$$

The *Fréchet Inception Distance* is an application of the Fréchet distance on the representation distributions from a specified model. The models are Inception v3 in the image domain and SupervisedFCN in the time series domain.

In [40] they argue that since the Gaussian distribution is the maximum entropy distribution over $\mathbb{R}^n$ for a given mean and covariance it is a reasonable distribution to assume for the representations. The mean and covariance is estimated from the samples and the explicit formula **??** is used to calculate the FID.

FID is not without fault, and the Gaussian assumption has been shown not to hold [42]. Further, as the FID relies on estimating large covariance matrices, a large number of samples is needed to obtain a reliable estimate.

Rethinking FID: [42]

[43] FID and IS are biased.

FID score measures difference in the distribution of representations of time series. The representations capture high level semantics of the time series and analyses of these representations can provide greater insights to the realism of

generated samples.

Classification Accuracy Score (CAS)

A method for evaluating the models ability to learn class conditional distributions is to train a separate classifier on the on synthetic data and test on real data (TSTR). That is we generate N synthetic samples $\{x_i, y_i\}_{i=1}^{N}$ using class conditional sampling. We then train a classifier on this synthetic dataset, and evaluate the CAS of this classifier on a real test dataset. High CAS values indicate that the generative model produces samples similar to the real data and captures relevant class specific features.

We evaluate the CAS for TSTR by using the Supervised FCN introduced in [1] on all our models considered and compare against the baseline model to investigate the relative performance.

Chapter 3

Related Work

TODO: relate our work to TimeVQVAE, Neural Representation, Barlow, MaskGIT,

TODO: Include something on time series generation / representation learning

3.1 MaskGIT

The Masked Generative Image Transformer (MaskGIT)[29] is a generative transformer model for image synthesis developed by Google Research. The novelty of the model lies in the token generation. Unlike popular autoregressive generative transformers, who treat images as a sequence of tokens, MaskGIT introduces an image synthesis paradigm using a bi-directional transformer decoder. This means that during training MaskGIT learns to predict tokens in all directions, an intuitively more natural way to consider images. At inference time MaskGIT starts out with a blank canvas and predicts the entire image, and iteratively keeps and conditions on the most confident pixels.

MaskGIT assumes a tokenization procedure for stage 1. In the original paper [29] VQGAN [44] was used and the actual contribution of the work revolved around improving stage 2, hence we present that part only.

3.1.1 Masked Visual Token Modeling (Prior learning)

For some image X in the dataset $\mathcal{D}$, let $Y = \{y_i\}_{i=1}^N$ denote the latent tokens obtained by passing X through the VQ-Encoder and denote the corresponding binary mask by $M = \{m_i\}_{i=1}^N$. During training a subset of Y is replaced by a special masking token we denote by $\mathtt{M}$ according to the binary mask M. This is done by

$$Y_{\text{Mask}} = Y \odot (1_N - M) + M \cdot \mathtt{M}, \tag{3.1}$$

where $\odot$ is the Hadamard product, i.e point wise multiplication, and 1_N is a vector with the same shape as M and Y.

The sampling procedure, or choice number of tokens to mask, is parameterized by a mask scheduling function γ. The sampling can be summarized as follows

- Sample $r \sim U(0,1]$.
- Sample $\lceil \gamma(r) \cdot N \rceil$ indices I uniformly from $\{0,\dots,N-1\}$ without replacement.
- Create M by setting $m_i = 1$ if $i \in I$, and $m_i = 0$ otherwise.

The training objective is to minimize the negative log likelihood of the masked tokes, conditional on the unmasked

$$\mathcal{L}_{\text{Mask}} = -\mathbb{E}_{Y \in \mathcal{D}} \left[\sum_{i \in I} p(y_i | Y_{\text{Mask}}) \right] \tag{3.2}$$

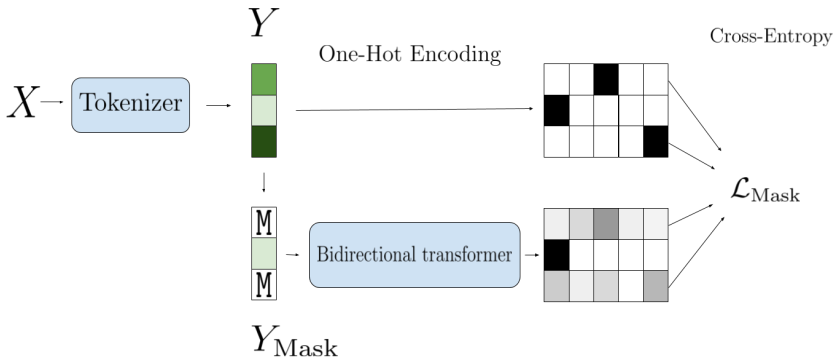

Figure 3.1: MaskGIT forward computation.

A bidirectional transformer is used to predict the probabilities $p(y_i|Y_{\text{Mask}})$ of each masked token, and $\mathcal{L}_{\text{Mask}}$ is computed as the cross entropy between the ground truth one-hot token and the predicted token.

3.1.2 Iterative decoding (Image generation)

The bi-directional transformer could in principle predict all `M` tokens and generate a sample in a single pass by simply sampling from the predicted probabilites $p(y_i|Y_{\text{Mask}})$ from a forward pass of an all masked sequence. However, there are challenges with this approach. In their original article [29] proposes a novel non-autoregressive decoding method to sythesize samples in a constant number of steps.

The decoding process goes from $t = 0$ to T. To generate a sample at inference time one starts out with a all masked sequence which we denote by $Y^{(0)}_{\text{Mask}}$. At it-

eration t the model predicts the probabilities for all the mask tokens, $p(y_i|Y^{(t)}_{\text{Mask}})$, in parallel. At each masked index i a token $y_i^{(t)}$ is sampled according to the predicted distribution, and the corresponding probability $c_i^{(t)}$ is used as a measure of the confidence in the sample. For the unmasked tokens a confidence of 1 is assigned to the true position. The number of $y_i^{(0)}$ with highest confidence kept for the next iteration is determined by the mask scheduling function. We mask $n = \lceil \gamma(t/T) \cdot N \rceil$ of the lower confidence tokens by calculating $M^{(t+1)}$ by

$$m_i^{(t+1)} = \begin{cases} 1, \text{ if } c_i < \text{Sort}([c_1^{(t)}, \ldots, c_N^{(t)}])[n] \\ 0, \text{ otherwise} \end{cases} \tag{3.3}$$

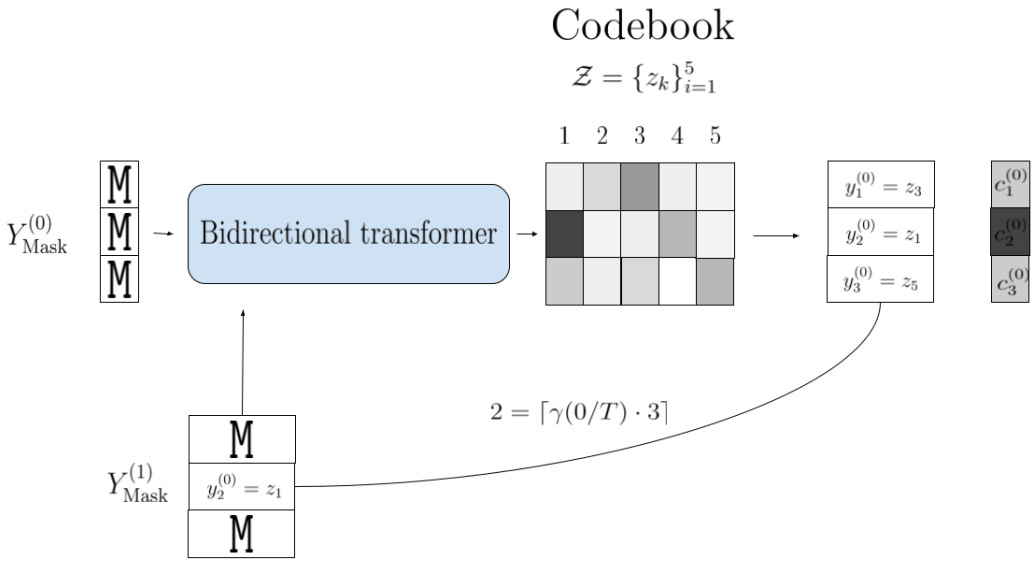

Figure 3.2: Illustration of first pass of the iterative decoding algorithm.

The algorithm synthesizes a full image in T steps.

Implementation details

3.2 TimeVQVAE

TimeVQVAE is a time series generation model based on VQVAE and MaskGIT. It is the first to our and the authors knowledge that utilizes vector quantization (VQ) to address the TSG problem. It leverages a two stage approach similar to VQVAE and uses a bidirectional transformer akin to MaskGIT for prior learning. Additionally, they propose VQ modeling in time-frequency domain, separating data into high

and low frequency components to better retain temporal consistencies and generate higher quality samples.

TimeVQVAE provides class-guided conditional sampling.

3.2.1 Tokenization

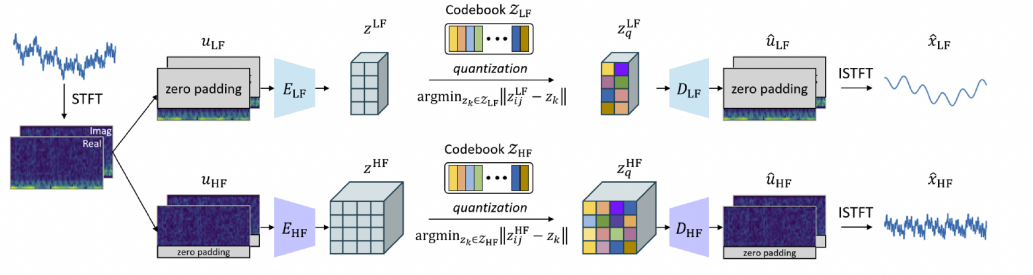

Figure 3.3: Stage 1: Tokenization. Figure taken with permission from [1]

3.2.2 Prior learning

TimeVQVAE uses a modified version of MaskGIT in order to learn the prior. As the original MaskGIT has no means of jointly sample from the two modalities introduced by the high-low frequency split.

For some X in the dataset $\mathcal{D}$, let $Y = \{y_i\}_{i=1}^N$ denote the latent tokens obtained by passing X through the VQ-Encoder and denote the corresponding binary mask by $M = \{m_i\}_{i=1}^N$.

A discrete latent representation $z_q \in \mathbb{R}^{d \times h \times w}$ can equivalently be represented as a sequence of codebook indices by

$$s_{ij} = k, \text{ whenever } (z_q)_{ij} = z_k \tag{3.4}$$

Class Conditional Sampling

3.3 SSL

Our model leverages SSL algorithms in order to learn more expressive latent representations. Here we present the relevant algorithms for our work, Barlow Twins and VIbCReg.
One fundamental difference between Barlow Twins and VIbCReg is that the branches are regularized differently. In Barlow Twins the regularization is applied to the

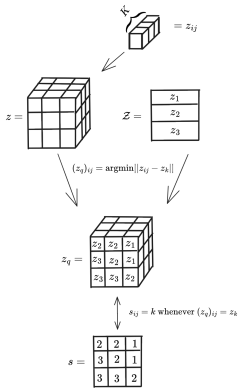

cross correlation matrix of the projected output of the two branches, which in general favours scenarios where the two branches produces similar summary statistics. In VIbCReg the covariance term is applied on each branch separately, which works better in scenarios where the branches are different [45].

3.3.1 Barlow Twins

Barlow Twins is a non-contrastive SSL method based on applying the *redundancy-reduction principle* (or efficient coding hypothesis) [46] from the neuroscientist H. Barlow to a pair of identical networks.

In essence the model wants to encourage representations of similar samples to be similar, while simultaneously reducing the amount of redundancy between the components of the vectors. This is enforced by producing two augmented views of each sample and projecting the their representations onto a vast feature space, in such a way that their cross-correlation is close to the identity.

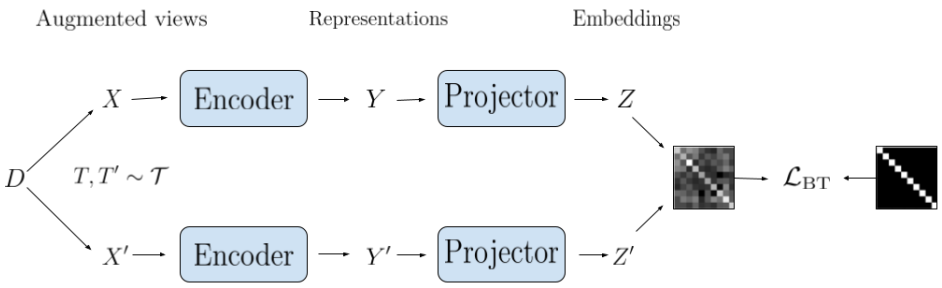

Figure 3.4: Overview of the Barlow Twins architecture. Figure inspired by [47]

The Barlow Twins algorithm starts out by creating two different augmented views for each datapoint in a batch D. The augmentations are selected by sampling from a collection of augmentations $\mathcal{T}$. We denote the batches of augmented views

$T(D) = X$ and $T'(D) = X'$, for augmentations $T, T' \sim \mathcal{T}$. The batches are then passed through an encoder (give representations Y and Y') and a *projector* to produce batches of embeddings Z and Z'. The embeddings are assumed to be mean centered across the batch dimension.

The loss function is calculated using the cross correlation matrix $\mathcal{C}$ between Z and Z', and measuring its deviance from the identity. In particular the Barlow Twins loss is defined as

$$\mathcal{L}_{\text{BT}} = \overbrace{\sum_i (1 - \mathcal{C}_{ii})^2}^{\text{Invariance}} + \lambda \overbrace{\sum_i \sum_{j \neq i} \mathcal{C}_{ij}^2}^{\text{Redundancy reduction}}, \tag{3.5}$$

where

$$\mathcal{C}_{ij} = \frac{\sum_b z_{b,i} z'_{b,j}}{\sqrt{\sum_b (z_{b,i})^2} \sqrt{\sum_b (z'_{b,j})^2}}. \tag{3.6}$$

The *invariance term* assists in making the embedding invariant to the distortions introduced by the augmentations, hence pushes the representations closer together. The *redundancy reduction term* decorrelates the different vector components, which reduces the information redundancy.

3.3.2 VIbCReg

VIbCReg [**lee2024vibcreg**] is a non-contrastive SSL model with siamese architecture based on VICReg [45]. It can be seen as VICReg with better covariance regularization and IterNorm [48]. Overall the architecture is similar to Barlow Twins, but a key difference is that variance/covariance regularization is done in each branch individually.

define or elaborate on this

As before a batch D is augmented to create two views and passed through an encoder and projector. The embedding Z and Z' are *whitened* using IterNorm [48].

The loss consists of a similarity loss between the branches, and feature decoration (FD) loss together with a feature component expressiveness (FcE) term at each branch. Input data is processed in batches. Let $Z \in \mathbb{R}^{B \times F}$ where B and F denotes the batch and feature sizes respectively. We denote a row in Z by Z_b and column by Z_f, and similarly for Z'.

The similarity loss is defined as the MSE of the two embeddings

$$s(Z, Z') = \frac{1}{B} \sum_{b=1}^{B} ||Z_b - Z'_b||_2^2, \tag{3.7}$$

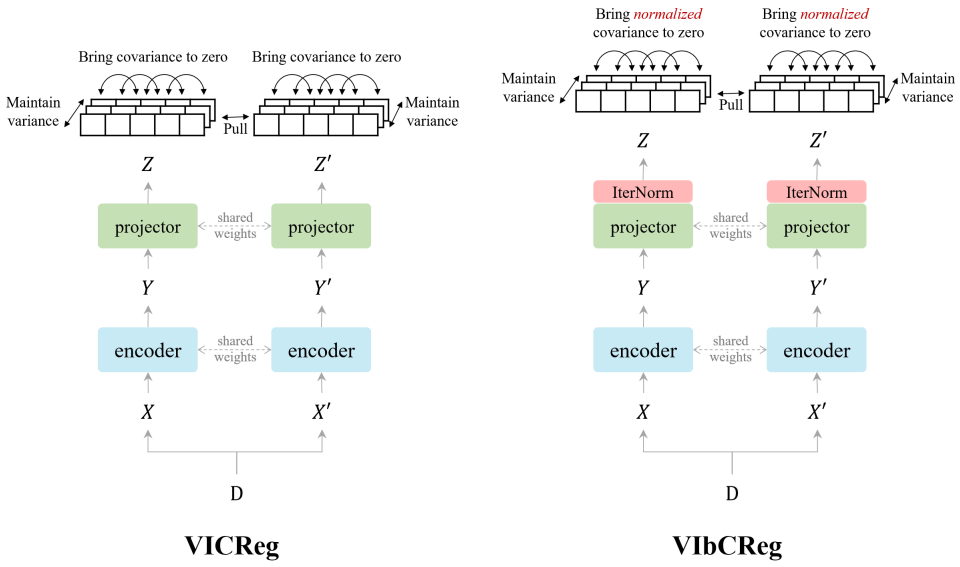

Figure 3.5: Overview of VIbCReg, and comparison with VICReg. Taken with permission from [19]

which encourages them to be similar. The FcE term acts on each branch separately and encourages the variation across a batch to stay at a specified level γ. It is defined as

$$v(Z) = \frac{1}{F}\sum_{f=1}^{F} \max(0, \gamma - \sqrt{\text{Var}(Z_f) + \epsilon}), \tag{3.8}$$

where Var() is a variance estimator, γ is a target value for the standard deviation, which both in VIbCReg and VICReg is set to 1. ϵ is a small scalar preventing numerical instabilities.
For the FD loss we first mean shift and normalize along the batch dimension

$$\widehat{Z}_b = \frac{Z_b - \bar{Z}}{||Z_b - \bar{Z}||_2} \text{ where } \bar{Z} = \frac{1}{B}\sum_{b=1}^{B} Z_b, \tag{3.9}$$

$$\widehat{Z} = [\widehat{Z}_1, ..., \widehat{Z}_B]^T, \tag{3.10}$$

compute the normalized covariance matrix

$$C(Z) = \frac{1}{B-1}\widehat{Z}^T\widehat{Z}, \tag{3.11}$$

and take the mean square across all off-diagonal elements to obtain the FD loss

$$c(Z) = \frac{1}{F^2}\sum_{i\neq j} C(Z)_{ij}^2. \tag{3.12}$$

The total loss is then given by

$$\mathcal{L}_{\text{VIbCReg}} = \lambda s(Z, Z') + \mu[v(Z) + v(Z')] + \nu[c(Z) + c(Z')] \tag{3.13}$$

where λ, μ and ν are hyperparameters determining the importance of each term. The normalization of the covariance matrix keeps the range of the FD loss small, independent of data, and eases hyperparameter tuning across datasets.

Chapter 4

Methodology

Our work in this thesis can be seen as a tangent of the paper "Vector Quantized Time Series Generation with a Bidirectional Prior Model" [1]. We simplify the model architecture by omitting the high-low frequency split, which reduces the model to what they refer to as "naive TimeVQVAE" in their paper. We expand on naive TimeVQVAE with a self-supervised extension.

A schematic figure of our proposed tokenization model is given in **??**. To improve on the reconstruction we add a regularizing term by reconstructing augmented views. We hypothesize that the model generalizes better to unseen data by letting the decoder "see" the augmented views.
To separate classes better we introduce a non contrastive self supervised loss. The intuition being that the representation of original and augmented views are pushed closer together by the SSL loss. We further enforce this hypothesis by using augmentations that preserve the overall semantics of the class conditional distributions.

4.1 Proposed model: NC-VQVAE

Our model, termed NC-VQVAE, is a generative time series model which learns expressive discrete latent representations by combining VQVAE [18] with non contrastive self supervised learning algorithms. NC-VQVAE uses the two staged modelling approach presented in [1], and can be considered an extension of their "naive TimeVQVAE". Our model mainly extends the tokenization stage, where we incorporate Barlow Twins [47] and VIbCReg [19] as our non contrastive SSL, but the framework is flexible. For stage two we model the prior using a bidirectional transformer as MaskGIT [29].

4.1.1 NC-VQVAE

The architecture of the tokenization model **??** consists of two branches. The top and bottom branch is referred to as the original and augmented branch respectively. The model takes a time series x as input and creates an augmented view x'. The original branch is simply the naive TimeVQVAE from [1], while the augmented branch is an autoencoder, constructed by omitting the quantization layer. The views are passed through their respective branches, where we compute the SSL loss derived from the original discrete latent representation z_q and the augmented continuous latent z', before the decoder reconstructs each latent representation. The SSL loss is calculated by concatenate the average and max pool of both representations individually and pass the resulting vectors to the projector.

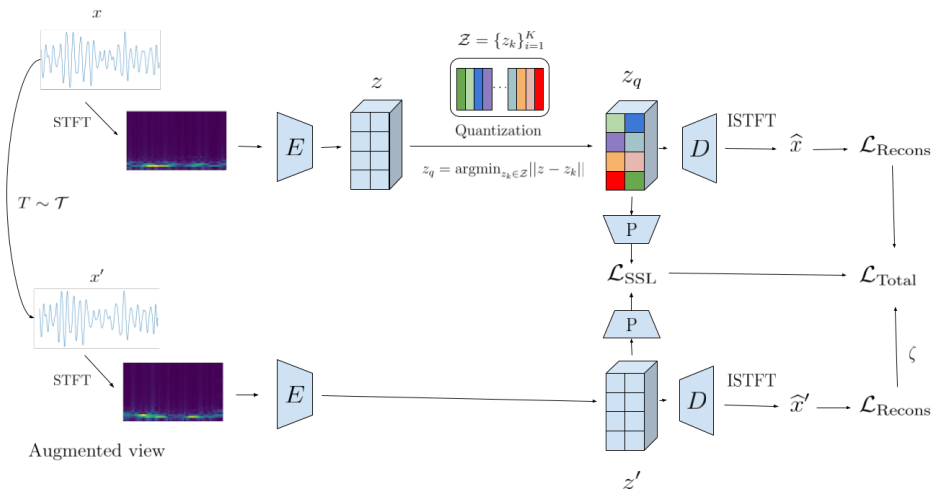

Figure 4.1: Overview of proposed model. NC-VQVAE

For prior learning we follow MaskGIT and refer to related works for a description of the learning and generation procedure.

Chapter 5

Experiments

5.1 Implementation details

We follow [1] closely in the encoder/decoder/codebook implementation, and

Time Frequency Modelling

The short time fourier transform (STFT) and its inverse ISTFT are implemented with `torch.stft` and `torch.istft` respectively. We follow [1] and set the main parameter `nfft` to 8, and use default parameters for the rest.

Encoder and decoder

Appendix C.3 from [1]
The same encoder and decoder architecture as in [18] is used and further use the implementation from [49] with adaptations from [1].
The encoder consists of n downsampling convolutional blocks (Conv2d - BatchNorm2d - LeakuReLU), followed by m residual blocks (LeakuReLU - Conv2d - BatchNorm2d - LeakuReLU - Conv2d). The downsampling convolutional layers are implemented with parameters kernel size=(3,4), stride=(1,2), padding=(1,1), while the residual convolutional layers have parameters kernel size=(3,3),stride=(1,1), padding=(1,1).
The decoder is implemented similarity with m resudial followed n upsampling layers using transposed convolutional layers with same parameters as in the encoder.
The downsampling rate is determined by 2^n where n is set such that z has width of 32.

VQ

Implementation from lucidrains/vector-quantize-pytorch. https://github.com/lucidrains/vector-quantize-pytorch

Codebook size $= 32$ and dimension $= 64$.
Use exponential moving average with decay 0.9, and commitment loss with weight $\beta = 1$.

Augmentations

window warp: window ratio: 0.4,min window warp: 0.9, max windowwarp: 2.0
amplitude resize: Amp Rrate: 0.2
gaussian noise: gaus mean: 0, gaus std: 0.05
slice and shuffle:

Projector

We follow the implementation from [19] for both Barlow Twins and VIbCReg.
Barlow Twins: Projector's dimension size is set to 4096. λ is set to $5 \cdot 10^3$.
VIbCReg: The dimension of the the projector is set to 4096. λ and μ are both set to 25, while ν is set to 100.

Prior learning

The number of iterations in the iterative decoding algorithm T, is set to 10, following [29]. We too use the cosine as mask scheduling function γ. The implementation is adopted from [1].

Optimizer

The AdamW optimizer with batch sizes for stage1: 128 and stage2: 256, initial learning rate 10^{-3}, cosine learning rate scheduler and weight decay of 10^{-5}. We run 1000 epochs for both stage 1 and 2.

Evaluation

KNN and SVM are implemented using scikit-learn. $K = 5$ in KNN and linear kernel in SVM.
FCN for IS, FID and CAS

5.2 Initial Experimentation and Model Development

The overarching objective in creating our model is to learn more expressive latent representations for better time series generation. We want to improve the reconstruction capabilities of the tokenization model. The rationality is that if the tokenization model reconstructs well the latent representations contains all relevant information of the input. We simultaneously want enforce better class separability in the latent representations, as we hypothesize that such additional

structure eases/improved learning of the generative model.

During development we encountered several problems:
When we attempted a siamese architecture, with quantization in the augmented branch, and to derive the SSL loss from the discrete representations there were a correlation problem. The codewords were very highly correlated, which resulted from the passing both views through the VQ. $SSL(z_q, z'_q)$
In an attempt to solve this we attempted to derive the SSL loss from the continuous latent representations, but the resulting discrete latent representations performed poorly on the downstream classification task. Separability problem: $SSL(z, z')$
The solution was to remove the VQ in the augmented branch and rather derive the SSL loss from z_q and z'. Solution: $SSL(z_q, z')$

Overfitting problem: Using $SG()$ on augmented branch / Not using augRecons

5.3 Main Experiments

We are primarily interested in two things. For stage 1, if NC-VQVAE learns more expressive representations, i.e are we able to reconstruct on par with VQVAE while simultaneously improve on downstream classification. For stage 2 we are interested in the effect NC-VQVAE has on prior learning and time series generation.

We evaluate our model NC-VQVAE with both Barlow Twins and VIbCReg as SSL method against the naive VQVAE as described in [1]. Firstly we look at the tokenization models, evaluating the reconstruction capability and performance on downstream classification. Then we train a prior model on top of the different tokenization models and evaluate the performance of the generative models by IS, FID, CAS and visual inspection.

5.4 Stage 1

5.4.1 Augmentations

In our experiments we consider three sets of augmentations with different characteristics. They are

- Amplitude Resizing + Window Warp
- Slice and Shuffle
- Gaussian noise

Amplitude Resizing + Window Warp scales in both x and y direction. The window warp has similar qualities to phase shift, but not uniformly and keeps endpoints fixed. They were considered as the observed conditional distribution in

some datasets, such as ShapesALL, had similar overall shape, but peaked with different amplitude and at different locations. Thus the augmented view had similar characteristics as the conditional distribution of the original view.

Slice and Shuffle crops the time series into three sections and permutes them. For datasets with sharp modularity and few peaks, such as ElectricDevices, the augmentation provides a view with peaks occurring at timestamps not seen in the training data, which could improve the reconstruction on unseen data, as well as encouraging the model to focus more on the existence of a peak rather than its specific location. For some datasets such as FordA, the semantics of the dataset is preserved under this augmentation, despite their continuous nature.

Gaussian noise adds a nose $\epsilon \sim N(0, 0.05)$ to each datapoint in the time series. This introduces, in many cases, a substantial high frequency component. As the naive VQVAE described in [1] had trouble with reconstruction of HF components, this augmentation could provide more emphasis on these. The reconstruction of the augmented views can too provide more information regarding HF components for the decoder.

5.4.2 Evaluation

Reconstruction, Classification and Visual inspection

5.5 Stage 2

5.5.1 Evaluation

- **IS**:
- **FID**:
- **CAS**:We evaluate the CAS for TSTR by using the Supervised FCN on all our models considered and compare against the baseline model to investigate the relative performance.
- **Visual inspection**:
- **Token usage**:

5.6 UCR Time Series Classification Archive

The evaluation of our model NC-VQVAE is done on a subset of the UCR Time Series Archive [50]. The UCR archive is a collection of 128 datasets of univariate time series for time series classification. The different datasets in the archive span a wide range characteristics, sensor, device, image-derived, simulated, . Each dataset has a predefined training and test split.

Our subset of the UCR archive is

TODO: Table of datasets

Type	Name	Train	Test	Class	Length
Type1	StarLightCurves	Train1	Test1	Class1	Length1
Type2	Name2	Train2	Test2	Class2	Length2
Type3	Name3	Train3	Test3	Class3	Length3
Type4	Name4	Train4	Test4	Class4	Length4
Type5	Name5	Train5	Test5	Class5	Length5

Table 5.1: Sample table with columns: Type, Name, Train, Test, Class, and Length.

"StarLightCurves", "Wafer", "ECG5000", 'SonyAIBORobotSurface1', 'SonyAIBORobotSurface2', "ElectricDevices", "TwoPatterns", "FordA", "UWaveGestureLibraryAll", "FordB", "ShapesAll", 'Symbols', 'Mallat'

Chapter 6

Results and Discussion

6.1 Stage 1

6.1.1 Reconstruction

6.1.2 Classification

6.2 Stage 2

6.2.1 Thought:

Better inception score and CAS of our models indicate that the class separability learned in latent space makes the conditional distributions more distinct easier to classify. The FID is variable, but in many cases better, which indicated that the generative distributions are closer to the ground truth.

Gaussian noise aug seems to result in a lot easier the BT/VIbCReg loss to minimize.
Slice and shuffle is harder to minimize, but could seem to push representations for different classes further apart resulting in better linear probes.

6.2.2 Ablation

6.2.3 Augmentation Reconstruction Weight

Here are the results of the ablation on the effect of "Augmentation Reconstruction Weight" on Stage 1. "Augmentation Reconstruction Weight" is the weight given to the reconstruction loss on the augmented branch. Tested weights 0.05, 0.1, 0.15 and 0.2. Augmentations [Window Warp, Amplitude Resize] and [Slice and Shuffle]. The weight has little effect on linear probe accuracy across the four datasets tested, and the two sets of augmentations. The effect on Validation reconstruction loss is small for all except FordA. It seems, not very surprisingly, that

the choice of augmentations are of (much) greater importance.

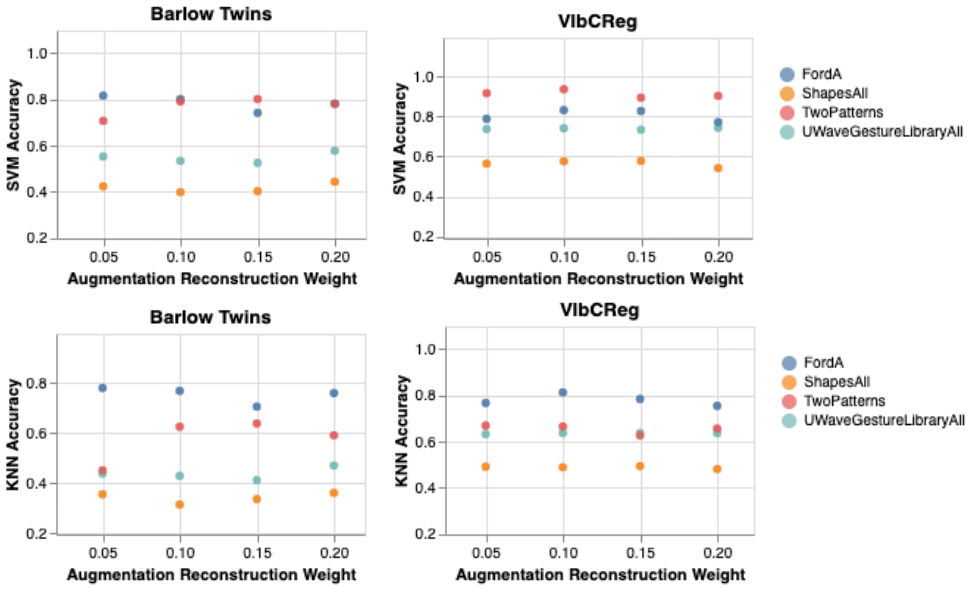

Figure 6.1: Augmentations: Window Warp and amplitude resize. Averaged across 2 runs. Trained for 250 epochs

6.2.4 Augmentation robustness

S1 - S2 - Augs: Choose datasets such that half were thought to be well fitting for slice and shuffle and half for amplitude resize + window Warp. This was after seeing FordA performing well with S and S, and looking at the augmented views.
FordA/B, Electric devices, ShapesALL for S and S
TwoP, UWave, symbols, Mallat for ampRes + winwarp

Visual inspection: Plot training samples + spectrogram, compare to augmented view. Compare these against others from other classes.
Does the resulting improvement in stage 1 transfer to stage 2?

TODO: Download the Wandb data.

Plot for each dataset and each augmentation: Color code according to SSL-model.

6.3 Discussion

The added flexibility of NC-VQVAE, with possibility of choosing dataset specific augmentations, can in some applications be beneficial.

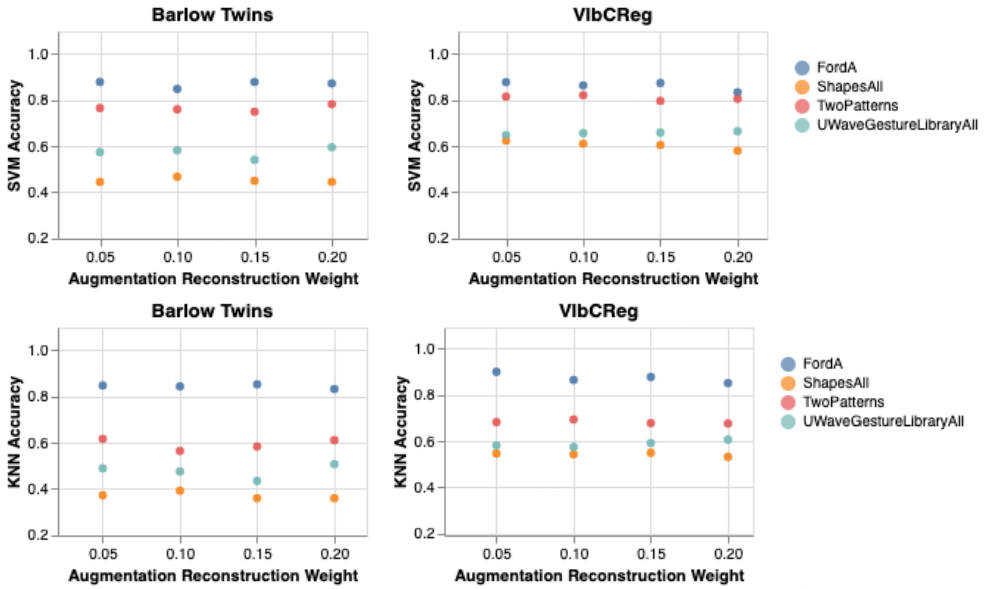

Figure 6.2: Augmentation: Slice and shuffle. Averaged across 2 runs. Trained for 250 epochs

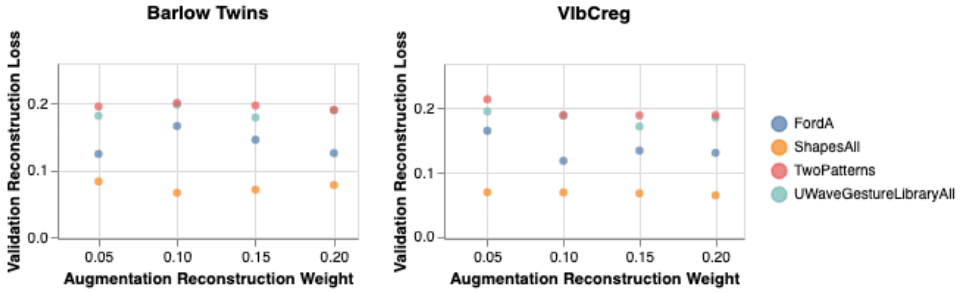

Figure 6.3: Augmentation: Window Warp and amplitude resize. Averaged across 2 runs. Trained for 250 epochs

6.4 Further work

[21] suggest that focus on augmentations is of great importance. The hunt for good augmentations in the time series domain is ongoing and should probably get more attention.
HF-LF split - augmentations tailored for HF and LF, as they often have quite different semantics.

Further optimize the relationship between aug recon loss and choice of augmentations.

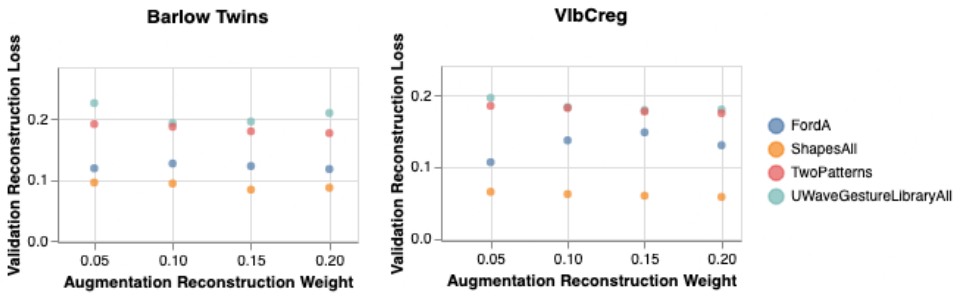

Figure 6.4: Augmentation: Slice and shuffle. Averaged across 2 runs. Trained for 250 epochs

Chapter 7

Conclusion

7.1 Reconstruction

7.2 Classification

Bibliography

[1] D. Lee, S. Malacarne and E. Aune, *Vector quantized time series generation with a bidirectional prior model*, 2023. arXiv: 2303.04743 [cs.LG].

[2] W. S. McCulloch and W. Pitts, 'A logical calculus of the ideas immanent in nervous activity,' *Bulletin of Mathematical Biology*, vol. 52, no. 1, pp. 99–115, 1990, ISSN: 0092-8240. DOI: https://doi.org/10.1016/S0092-8240(05)80006-0. [Online]. Available: https://www.sciencedirect.com/science/article/pii/S0092824005800060.

[3] F. Rosenblatt, *The Perceptron, a Perceiving and Recognizing Automaton Project Para*, ser. Report: Cornell Aeronautical Laboratory. Cornell Aeronautical Laboratory, 1957. [Online]. Available: https://books.google.no/books?id=P_XGPgAACAAJ.

[4] K. Hornik, M. Stinchcombe and H. White, 'Multilayer feedforward networks are universal approximators,' *Neural Networks*, vol. 2, no. 5, pp. 359–366, 1989, ISSN: 0893-6080. DOI: https://doi.org/10.1016/0893-6080(89)90020-8. [Online]. Available: https://www.sciencedirect.com/science/article/pii/0893608089900208.

[5] I. Goodfellow, Y. Bengio and A. Courville, *Deep Learning*. MIT Press, 2016, http://www.deeplearningbook.org.

[6] D. H. Hubel and T. N. Wiesel, 'Receptive fields and functional architecture of monkey striate cortex,' *The Journal of Physiology*, vol. 195, no. 1, pp. 215–243, 1968. DOI: https://doi.org/10.1113/jphysiol.1968.sp008455. eprint: https://physoc.onlinelibrary.wiley.com/doi/pdf/10.1113/jphysiol.1968.sp008455. [Online]. Available: https://physoc.onlinelibrary.wiley.com/doi/abs/10.1113/jphysiol.1968.sp008455.

[7] K. Fukushima, S. Miyake and T. Ito, 'Neocognitron: A neural network model for a mechanism of visual pattern recognition,' *IEEE Transactions on Systems, Man, and Cybernetics*, vol. SMC-13, no. 5, pp. 826–834, 1983. DOI: 10.1109/TSMC.1983.6313076.

[8] Y. LeCun, B. Boser, J. S. Denker, D. Henderson, R. E. Howard, W. Hubbard and L. D. Jackel, 'Backpropagation applied to handwritten zip code recognition,' *Neural Computation*, vol. 1, no. 4, pp. 541–551, 1989. DOI: 10.1162/neco.1989.1.4.541.

[9] J. Gu, Z. Wang, J. Kuen, L. Ma, A. Shahroudy, B. Shuai, T. Liu, X. Wang, L. Wang, G. Wang, J. Cai and T. Chen, *Recent advances in convolutional neural networks*, 2017. arXiv: 1512.07108 [cs.CV].

[10] Y. Bengio, A. Courville and P. Vincent, *Representation learning: A review and new perspectives*, 2014. arXiv: 1206.5538 [cs.LG].

[11] L. Jing and Y. Tian, *Self-supervised visual feature learning with deep neural networks: A survey*, 2019. arXiv: 1902.06162 [cs.CV].

[12] K. Nozawa and I. Sato, *Empirical evaluation and theoretical analysis for representation learning: A survey*, 2022. arXiv: 2204.08226 [cs.LG].

[13] A. Vaswani, N. Shazeer, N. Parmar, J. Uszkoreit, L. Jones, A. N. Gomez, L. Kaiser and I. Polosukhin, *Attention is all you need*, 2023. arXiv: 1706.03762 [cs.CL].

[14] A. Dosovitskiy, L. Beyer, A. Kolesnikov, D. Weissenborn, X. Zhai, T. Unterthiner, M. Dehghani, M. Minderer, G. Heigold, S. Gelly, J. Uszkoreit and N. Houlsby, *An image is worth 16x16 words: Transformers for image recognition at scale*, 2021. arXiv: 2010.11929 [cs.CV].

[15] S. Latif, A. Zaidi, H. Cuayahuitl, F. Shamshad, M. Shoukat and J. Qadir, *Transformers in speech processing: A survey*, 2023. arXiv: 2303.11607 [cs.CL].

[16] Q. Wen, T. Zhou, C. Zhang, W. Chen, Z. Ma, J. Yan and L. Sun, *Transformers in time series: A survey*, 2023. arXiv: 2202.07125 [cs.LG].

[17] Y. Bengio, P. Simard and P. Frasconi, 'Learning long-term dependencies with gradient descent is difficult,' *IEEE Transactions on Neural Networks*, vol. 5, no. 2, pp. 157–166, 1994. DOI: 10.1109/72.279181.

[18] A. van den Oord, O. Vinyals and K. Kavukcuoglu, 'Neural discrete representation learning,' *CoRR*, vol. abs/1711.00937, 2017. arXiv: 1711.00937. [Online]. Available: http://arxiv.org/abs/1711.00937.

[19] D. Lee and E. Aune, *Computer vision self-supervised learning methods on time series*, 2024. arXiv: 2109.00783 [cs.LG].

[20] J. Bromley, I. Guyon, Y. Lecun, E. Säckinger and R. Shah, 'Signature verification using a siamese time delay neural network.,' vol. 7, Jan. 1993, pp. 737–744.

[21] W. Morningstar, A. Bijamov, C. Duvarney, L. Friedman, N. Kalibhat, L. Liu, P. Mansfield, R. Rojas-Gomez, K. Singhal, B. Green and S. Prakash, *Augmentations vs algorithms: What works in self-supervised learning*, 2024. arXiv: 2403.05726 [cs.LG].

[22] K. He, H. Fan, Y. Wu, S. Xie and R. Girshick, *Momentum contrast for unsupervised visual representation learning*, 2020. arXiv: 1911.05722 [cs.CV].

[23] T. Chen, S. Kornblith, M. Norouzi and G. Hinton, *A simple framework for contrastive learning of visual representations*, 2020. arXiv: 2002.05709 [cs.LG].

[24] G. Mialon, R. Balestriero and Y. LeCun, *Variance covariance regularization enforces pairwise independence in self-supervised representations*, 2024. arXiv: 2209.14905 [cs.LG].

[25] J. Devlin, M.-W. Chang, K. Lee and K. Toutanova, *Bert: Pre-training of deep bidirectional transformers for language understanding*, 2019. arXiv: 1810.04805 [cs.CL].

[26] A. Radford and K. Narasimhan, 'Improving language understanding by generative pre-training,' 2018. [Online]. Available: https://api.semanticscholar.org/CorpusID:49313245.

[27] K. He, X. Chen, S. Xie, Y. Li, P. Dollár and R. Girshick, *Masked autoencoders are scalable vision learners*, 2021. arXiv: 2111.06377 [cs.CV].

[28] K. He, X. Zhang, S. Ren and J. Sun, *Deep residual learning for image recognition*, 2015. arXiv: 1512.03385 [cs.CV].

[29] H. Chang, H. Zhang, L. Jiang, C. Liu and W. T. Freeman, *Maskgit: Masked generative image transformer*, 2022. arXiv: 2202.04200 [cs.CV].

[30] S. Li, L. Zhang, Z. Wang, D. Wu, L. Wu, Z. Liu, J. Xia, C. Tan, Y. Liu, B. Sun and S. Z. Li, *Masked modeling for self-supervised representation learning on vision and beyond*, 2024. arXiv: 2401.00897 [cs.CV].

[31] D. P. Kingma and M. Welling, *Auto-encoding variational bayes*, 2022. arXiv: 1312.6114 [stat.ML].

[32] D. P. Kingma and M. Welling, 'An introduction to variational autoencoders,' *Foundations and Trends® in Machine Learning*, vol. 12, no. 4, pp. 307–392, 2019, ISSN: 1935-8245. DOI: 10.1561/2200000056. [Online]. Available: http://dx.doi.org/10.1561/2200000056.

[33] R. Gray, 'Vector quantization,' *IEEE ASSP Magazine*, vol. 1, no. 2, pp. 4–29, 1984. DOI: 10.1109/MASSP.1984.1162229.

[34] A. van den Oord, N. Kalchbrenner and K. Kavukcuoglu, *Pixel recurrent neural networks*, 2016. arXiv: 1601.06759 [cs.CV].

[35] A. van den Oord, S. Dieleman, H. Zen, K. Simonyan, O. Vinyals, A. Graves, N. Kalchbrenner, A. Senior and K. Kavukcuoglu, *Wavenet: A generative model for raw audio*, 2016. arXiv: 1609.03499 [cs.SD].

[36] Z. Wang, W. Yan and T. Oates, *Time series classification from scratch with deep neural networks: A strong baseline*, 2016. arXiv: 1611.06455 [cs.LG].

[37] T. Salimans, I. Goodfellow, W. Zaremba, V. Cheung, A. Radford and X. Chen, *Improved techniques for training gans*, 2016. arXiv: 1606.03498 [cs.LG].

[38] S. Barratt and R. Sharma, *A note on the inception score*, 2018. arXiv: 1801.01973 [stat.ML].

[39] A. Borji, *Pros and cons of gan evaluation measures: New developments*, 2021. arXiv: 2103.09396 [cs.LG].

[40] M. Heusel, H. Ramsauer, T. Unterthiner, B. Nessler and S. Hochreiter, *Gans trained by a two time-scale update rule converge to a local nash equilibrium*, 2018. arXiv: 1706.08500 [cs.LG].

[41] D. Dowson and B. Landau, 'The fréchet distance between multivariate normal distributions,' *Journal of Multivariate Analysis*, vol. 12, no. 3, pp. 450–455, 1982, ISSN: 0047-259X. DOI: https://doi.org/10.1016/0047-259X(82)90077-X. [Online]. Available: https://www.sciencedirect.com/science/article/pii/0047259X8290077X.

[42] S. Jayasumana, S. Ramalingam, A. Veit, D. Glasner, A. Chakrabarti and S. Kumar, *Rethinking fid: Towards a better evaluation metric for image generation*, 2024. arXiv: 2401.09603 [cs.CV].

[43] M. J. Chong and D. Forsyth, *Effectively unbiased fid and inception score and where to find them*, 2020. arXiv: 1911.07023 [cs.CV].

[44] P. Esser, R. Rombach and B. Ommer, *Taming transformers for high-resolution image synthesis*, 2021. arXiv: 2012.09841 [cs.CV].

[45] A. Bardes, J. Ponce and Y. LeCun, *Vicreg: Variance-invariance-covariance regularization for self-supervised learning*, 2022. arXiv: 2105.04906 [cs.CV].

[46] H. Barlow, 'Possible principles underlying the transformations of sensory messages,' *Sensory Communication*, vol. 1, Jan. 1961. DOI: 10.7551/mitpress/9780262518420.003.0013.

[47] J. Zbontar, L. Jing, I. Misra, Y. LeCun and S. Deny, *Barlow twins: Self-supervised learning via redundancy reduction*, 2021. arXiv: 2103.03230 [cs.CV].

[48] L. Huang, Y. Zhou, F. Zhu, L. Liu and L. Shao, *Iterative normalization: Beyond standardization towards efficient whitening*, 2019. arXiv: 1904.03441 [cs.CV].

[49] Y.-H.Huang, K. Huang and P. Fernández, *Vq-vae*, https://github.com/nadavbh12/VQ-VAE, 2021.

[50] H. A. Dau, E. Keogh, K. Kamgar, C.-C. M. Yeh, Y. Zhu, S. Gharghabi, C. A. Ratanamahatana, Yanping, B. Hu, N. Begum, A. Bagnall, A. Mueen, G. Batista and Hexagon-ML, *The ucr time series classification archive*, https://www.cs.ucr.edu/~eamonn/time_series_data_2018/, Oct. 2018.

Appendix A

Additional Material

Additional material that does not fit in the main thesis but may still be relevant to share, e.g., raw data from experiments and surveys, code listings, additional plots, pre-project reports, project agreements, contracts, logs etc., can be put in appendices. Simply issue the command `\appendix` in the main `.tex` file, and make one chapter per appendix.

If the appendix is in the form of a ready-made PDF file, it should be supported by a small descriptive text, and included using the `pdfpages` package. To illustrate how it works, a standard project agreement (for the IE faculty at NTNU in Gjøvik) is attached here. You would probably want the included PDF file to begin on an odd (right hand) page, which is achieved by using the `\cleardoublepage` command immediately before the `\includepdf[]{}` command. Use the option `[pages=-]` to include all pages of the PDF document, or, e.g., `[pages=2-4]` to include only the given page range.

NTNU

Vår dato Vår referanse

Norges teknisk-naturvitenskapelige universitet

Prosjektavtale

mellom NTNU Fakultet for informasjonsteknologi og elektroteknikk (IE) på Gjøvik (utdanningsinstitusjon), og

_____

_____ (oppdragsgiver), og

_____

_____

_____ (student(er))

Avtalen angir avtalepartenes plikter vedrørende gjennomføring av prosjektet og rettigheter til anvendelse av de resultater som prosjektet frembringer:

1. Studenten(e) skal gjennomføre prosjektet i perioden fra _____ til_____ .

   Studentene skal i denne perioden følge en oppsatt fremdriftsplan der NTNU IE på Gjøvik yter veiledning. Oppdragsgiver yter avtalt prosjektbistand til fastsatte tider. Oppdragsgiver stiller til rådighet kunnskap og materiale som er nødvendig for å få gjennomført prosjektet. Det forutsettes at de gitte problemstillinger det arbeides med er aktuelle og på et nivå tilpasset studentenes faglige kunnskaper. Oppdragsgiver plikter på forespørsel fra NTNU å gi en vurdering av prosjektet vederlagsfritt.

2. Kostnadene ved gjennomføringen av prosjektet dekkes på følgende måte:
   - Oppdragsgiver dekker selv gjennomføring av prosjektet når det gjelder f.eks. materiell, telefon/fax, reiser og nødvendig overnatting på steder langt fra NTNU på Gjøvik. Studentene dekker utgifter for ferdigstillelse av prosjektmateriell.
   - Eiendomsretten til eventuell prototyp tilfaller den som har betalt komponenter og materiell mv. som er brukt til prototypen. Dersom det er nødvendig med større og/eller spesielle investeringer for å få gjennomført prosjektet, må det gjøres en egen avtale mellom partene om eventuell kostnadsfordeling og eiendomsrett.

3. NTNU IE på Gjøvik står ikke som garantist for at det oppdragsgiver har bestilt fungerer etter hensikten, ei heller at prosjektet blir fullført. Prosjektet må anses som en eksamensrelatert oppgave som blir bedømt av intern og ekstern sensor. Likevel er det en forpliktelse for utøverne av prosjektet å fullføre dette til avtalte spesifikasjoner, funksjonsnivå og tider.

4. Alle bacheloroppgaver som ikke er klausulert og hvor forfatteren(e) har gitt sitt samtykke til publisering, kan gjøres tilgjengelig via NTNUs institusjonelle arkiv hvis de har skriftlig karakter A, B eller C.

Tilgjengeliggjøring i det åpne arkivet forutsetter avtale om delvis overdragelse av opphavsrett, se «avtale om publisering» (jfr Lov om opphavsrett). Oppdragsgiver og veileder godtar slik offentliggjøring når de signerer denne prosjektavtalen, og må evt. gi skriftlig melding til studenter og instituttleder/fagenhetsleder om de i løpet av prosjektet endrer syn på slik offentliggjøring.

Den totale besvarelsen med tegninger, modeller og apparatur så vel som programlisting, kildekode mv. som inngår som del av eller vedlegg til besvarelsen, kan vederlagsfritt benyttes til undervisnings- og forskningsformål. Besvarelsen, eller vedlegg til den, må ikke nyttes av NTNU til andre formål, og ikke overlates til utenforstående uten etter avtale med de øvrige parter i denne avtalen. Dette gjelder også firmaer hvor ansatte ved NTNU og/eller studenter har interesser.

5. Besvarelsens spesifikasjoner og resultat kan anvendes i oppdragsgivers egen virksomhet. Gjør studenten(e) i sin besvarelse, eller under arbeidet med den, en patentbar oppfinnelse, gjelder i forholdet mellom oppdragsgiver og student(er) bestemmelsene i Lov om retten til oppfinnelser av 17. april 1970, §§ 4-10.

6. Ut over den offentliggjøring som er nevnt i punkt 4 har studenten(e) ikke rett til å publisere sin besvarelse, det være seg helt eller delvis eller som del i annet arbeide, uten samtykke fra oppdragsgiver. Tilsvarende samtykke må foreligge i forholdet mellom student(er) og faglærer/veileder for det materialet som faglærer/veileder stiller til disposisjon.

7. Studenten(e) leverer oppgavebesvarelsen med vedlegg (pdf) i NTNUs elektroniske eksamenssystem. I tillegg leveres ett eksemplar til oppdragsgiver.

8. Denne avtalen utferdiges med ett eksemplar til hver av partene. På vegne av NTNU, IE er det instituttleder/faggruppeleder som godkjenner avtalen.

9. I det enkelte tilfelle kan det inngås egen avtale mellom oppdragsgiver, student(er) og NTNU som regulerer nærmere forhold vedrørende bl.a. eiendomsrett, videre bruk, konfidensialitet, kostnadsdekning og økonomisk utnyttelse av resultatene. Dersom oppdragsgiver og student(er) ønsker en videre eller ny avtale med oppdragsgiver, skjer dette uten NTNU som partner.

10. Når NTNU også opptrer som oppdragsgiver, trer NTNU inn i kontrakten både som utdanningsinstitusjon og som oppdragsgiver.

11. Eventuell uenighet vedrørende forståelse av denne avtale løses ved forhandlinger avtalepartene imellom. Dersom det ikke oppnås enighet, er partene enige om at tvisten løses av voldgift, etter bestemmelsene i tvistemålsloven av 13.8.1915 nr. 6, kapittel 32.

12. Deltakende personer ved prosjektgjennomføringen:

NTNUs veileder (navn): _____

Oppdragsgivers kontaktperson (navn): _____

Student(er) (signatur): _____ dato _____

_____ dato _____

_____ dato _____

_____ dato _____

Oppdragsgiver (signatur):_____ dato _____

Signert avtale leveres digitalt i Blackboard, rom for bacheloroppgaven.
Godkjennes digitalt av instituttleder/faggruppeleder.

Om papirversjon med signatur er ønskelig, må papirversjon leveres til instituttet i tillegg.
Plass for evt sign:

Instituttleder/faggruppeleder (signatur): _____ dato _____